DEPARTMENT OF PHYSICS · **UDESC**

SEMINAR · **2026**

RAY TRACING IN RELATIVISTIC STARS

From geometry to *observation*



How spacetime curvature decides the *image*, the *spectrum* and the *light curve* that an X-ray telescope receives from a neutron star.

$$\psi(b) = \int du \,/\, \sqrt{(b^{-2} - u^2(1 - R_s u))}$$ THE LIGHT LEAVING THE SURFACE

Rafael C. R. de Lima

Department of Physics · UDESC/CCT · Joinville, Brazil

rafael-lima.pages.dev/talks

OUTLINE

Four parts, *one path*

I

The star inside

What holds a neutron star up: the TOV equation, the equation of state and the mass–radius curve.

II

Relativistic ray tracing

Null geodesics in Schwarzschild: light bending, redshift and time delays — and how to follow the rays backwards, from the telescope to the surface.

III

Pulsars and neutron stars

The laboratories: pulsars and magnetars, hot spots, rotation, atmospheres — and what NICER has already measured.

IV

Recent results

My work: magnetar light curves, a massive low-field magnetar, accretion columns — and tests of alternative theories of gravity.

THE PREMISE

Everything we know arrives *as photons*

Compact stars are *natural laboratories* of strong-field gravity — but we know them only through the photons that left them and crossed a curved spacetime.

metric → null geodesics → image · spectrum · light curve → telescope → **M, R, field, gravity**

THE DIRECT PROBLEM

Given the star and the metric, predict what is observed. That is **ray tracing**.

THE INVERSE PROBLEM

Given what is observed, infer mass, radius, spot geometry and magnetic field.

THE TEST

If the metric is not Schwarzschild, the light curves change: observation tests **gravity**.

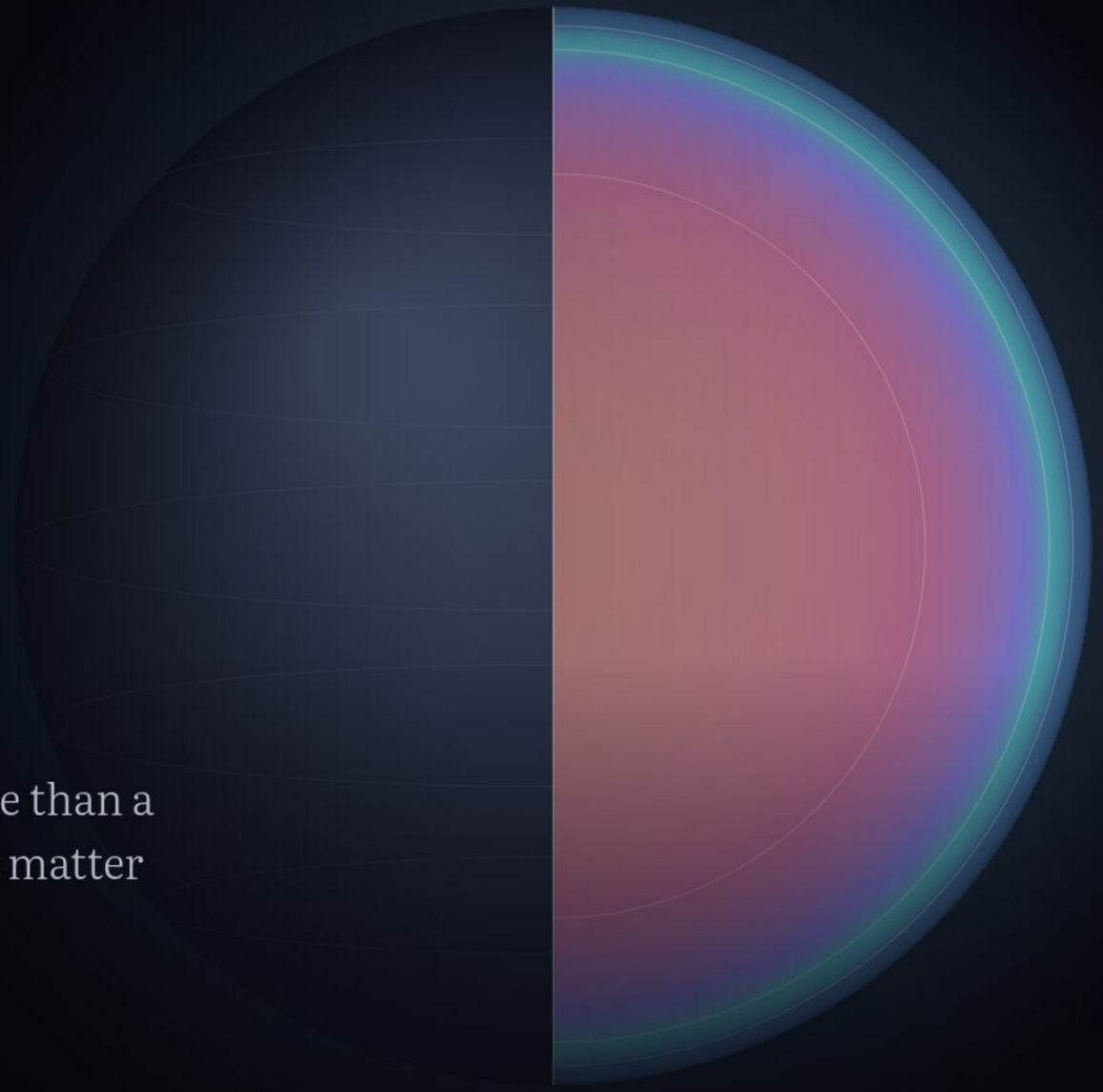
I

PART ONE

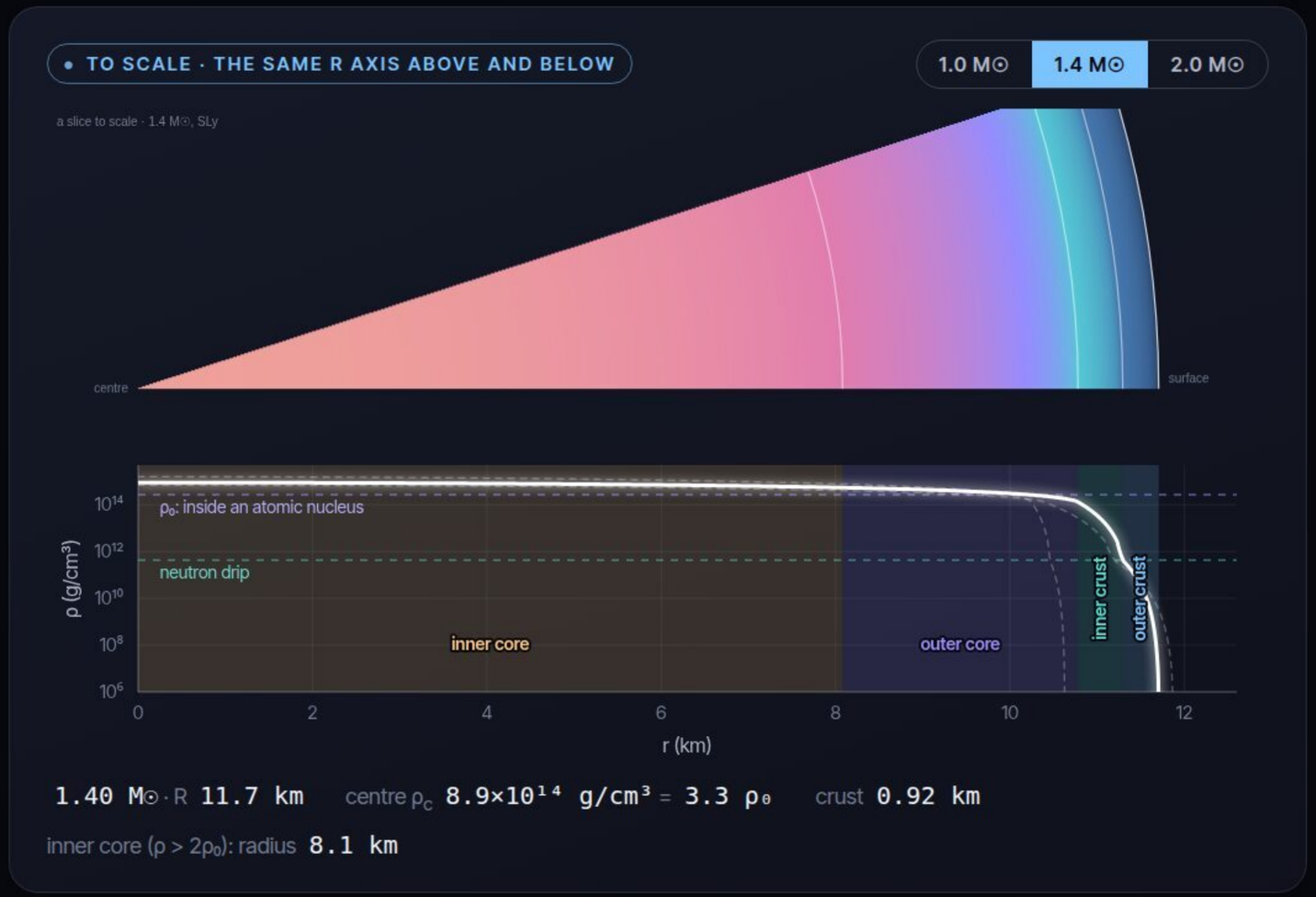
The star *inside*

Before following the light, the source: what holds more than a solar mass within 12 km — the pressure of the densest matter we know, against the gravity of general relativity.

anatomy · TOV equilibrium · equation of state · mass and radius



From the crust *to the unknown core*



- **Atmosphere and ocean**: centimetres to metres of H, He or C — where the light of Part II comes from.
- **Outer crust**: a lattice of ever more neutron-rich nuclei in a sea of electrons, up to 4×10^{11} g/cm³, when neutrons start to drip out of the nuclei.
- **Inner crust**: nuclei and free, superfluid neutrons; at the bottom, "nuclear pasta". Up to ~$\rho_0/2$.
- **Outer core**: neutrons, with some protons, electrons and muons, up to ~$2\rho_0$.
- **Inner core**: up to ~$6\rho_0$. Hyperons? Free quarks? The **equation of state** decides.

$\rho_0 = 2.7\times10^{14}$ g/cm³ is the density inside an atomic nucleus. TOV profile with SLy (Douchin & Haensel 2001, in the piecewise polytropes of Read et al. 2009).

TOLMAN · OPPENHEIMER & VOLKOFF · 1939

Hydrostatic equilibrium *in general relativity*

$$\frac{dP}{dr} = -\frac{Gm\rho}{r^2}$$

NEWTON · $dm/dr = 4\pi r^2\rho$

$$\frac{dP}{dr} = -\frac{Gm\rho}{r^2}\left(1+\frac{P}{\rho c^2}\right)\left(1+\frac{4\pi r^3 P}{mc^2}\right)\left(1-\frac{2Gm}{rc^2}\right)^{-1}$$

THE TOV EQUATION · $\rho c^2 = \varepsilon$, THE ENERGY DENSITY

PRESSURE HAS INERTIA

Pressure is energy, and energy resists acceleration like mass. At the centre of this star: **×1.15**

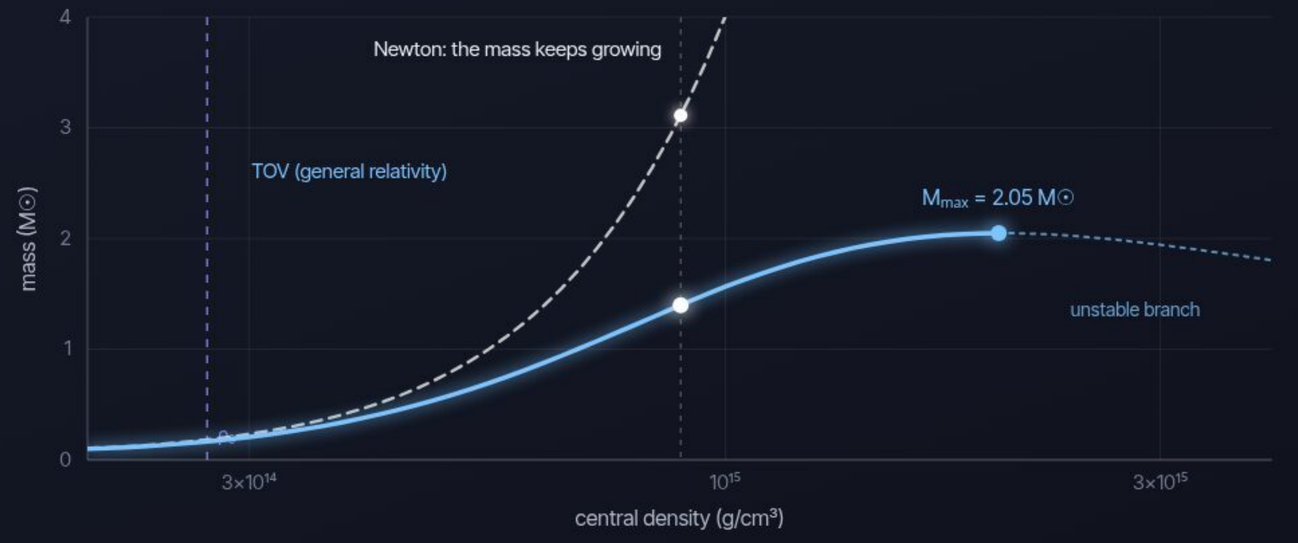
PRESSURE GRAVITATES

Pressure is also a source of gravity and adds to the mass. At the centre: **×1.46**

SPACE CURVES

Radial distances stretch, and the factor grows outwards. At the surface: **×1.54**

More pressure, more gravity: squeezing harder is not enough, and a **maximum mass** appears — which Newton does not have.



central density, ρ_c · SLy — 8.9×10^{14} g/cm³

TOV 1.40 M⊙, 11.7 km Newton 3.11 M⊙, 15.2 km at the centre $P/\rho c^2$ 0.154 $2GM/Rc^2$ 0.353

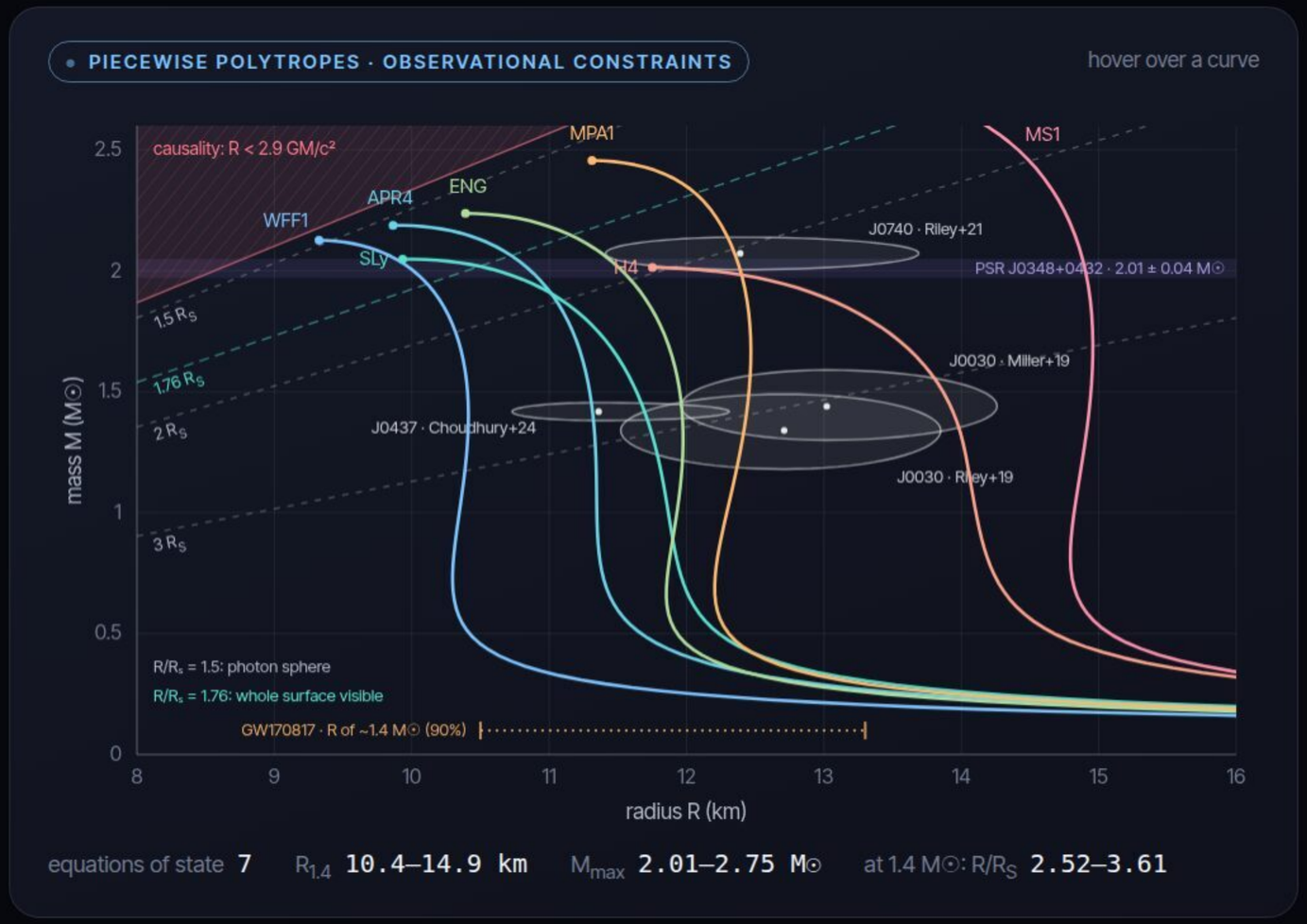
How hard matter *resists being squeezed*



- The equation of state gives the **pressure as a function of density**, P(ρ): what the TOV needs to close.
- Up to ~ρ_0 laboratory nuclear physics constrains the curve; above, each model extrapolates: two- and three-nucleon forces (WFF1, APR4), Skyrme (SLy), relativistic Brueckner–Hartree–Fock (ENG, MPA1), relativistic mean field (MS1; H4, with hyperons).
- **Stiff** — more pressure at the same density — gives a bigger, heavier star; **soft**, a smaller, lighter one.
- Limits: sound cannot outrun light, and 2 M☉ pulsars rule out the softest.

$c_s^2/c^2 = \Gamma P/(\varepsilon + P)$. The dot marks the centre of the maximum-mass star; beyond it, the curve is faded. The jumps come from the polytrope fit, which changes Γ at $10^{14.7}$ and 10^{15} g/cm³; near the centre of the heaviest stars some fits exceed *c*.

From nuclear physics *to the M–R curve*



$$\frac{dP}{dr} = -\frac{G(\varepsilon + P)(m + 4\pi r^3 P/c^2)}{c^2 r(r - 2Gm/c^2)}$$

RELATIVISTIC HYDROSTATIC EQUILIBRIUM (TOV)

Each equation of state P(ε) gives a mass–radius curve and a maximum mass. Measuring the **mass and radius of the same star** picks between them.

The lines of constant compactness look ahead to Part II: below R = 1.76 R_S the whole surface is in view; at 1.5 R_S lies the photon sphere.

Piecewise polytropes of Read, Lackey, Owen & Friedman (2009); constraints (68%): NICER — Riley et al. 2019, 2021; Miller et al. 2019; Choudhury et al. 2024; PSR J0348+0432 (Antoniadis et al. 2013); GW170817 (Abbott et al. 2018).

II

PART TWO

Relativistic *ray tracing*

Near a mass, light does not travel in a straight line: it follows the null geodesics of the metric. Ray tracing means following those geodesics backwards — from the telescope to the source.

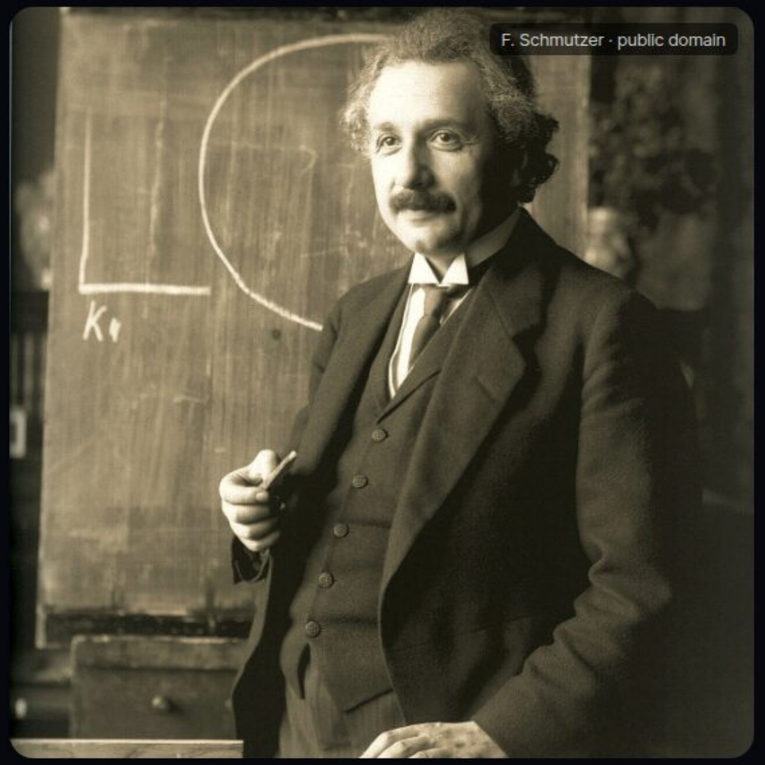
null geodesics · light bending · redshift · the image of a compact star · the recipe



SMACS 0723 (JWST) · NASA, ESA, CSA, STScI · public domain

25 NOVEMBER 1915

Einstein and *his field equations*



Albert Einstein
1921

$$G_{\mu\nu} = \frac{8\pi G}{c^4} T_{\mu\nu}$$

CURVATURE = ENERGY AND MOMENTUM CONTENT

$$\frac{d^2x^\mu}{d\lambda^2} + \Gamma^\mu{}_{\alpha\beta} \frac{dx^\alpha}{d\lambda} \frac{dx^\beta}{d\lambda} = 0$$

GEODESIC

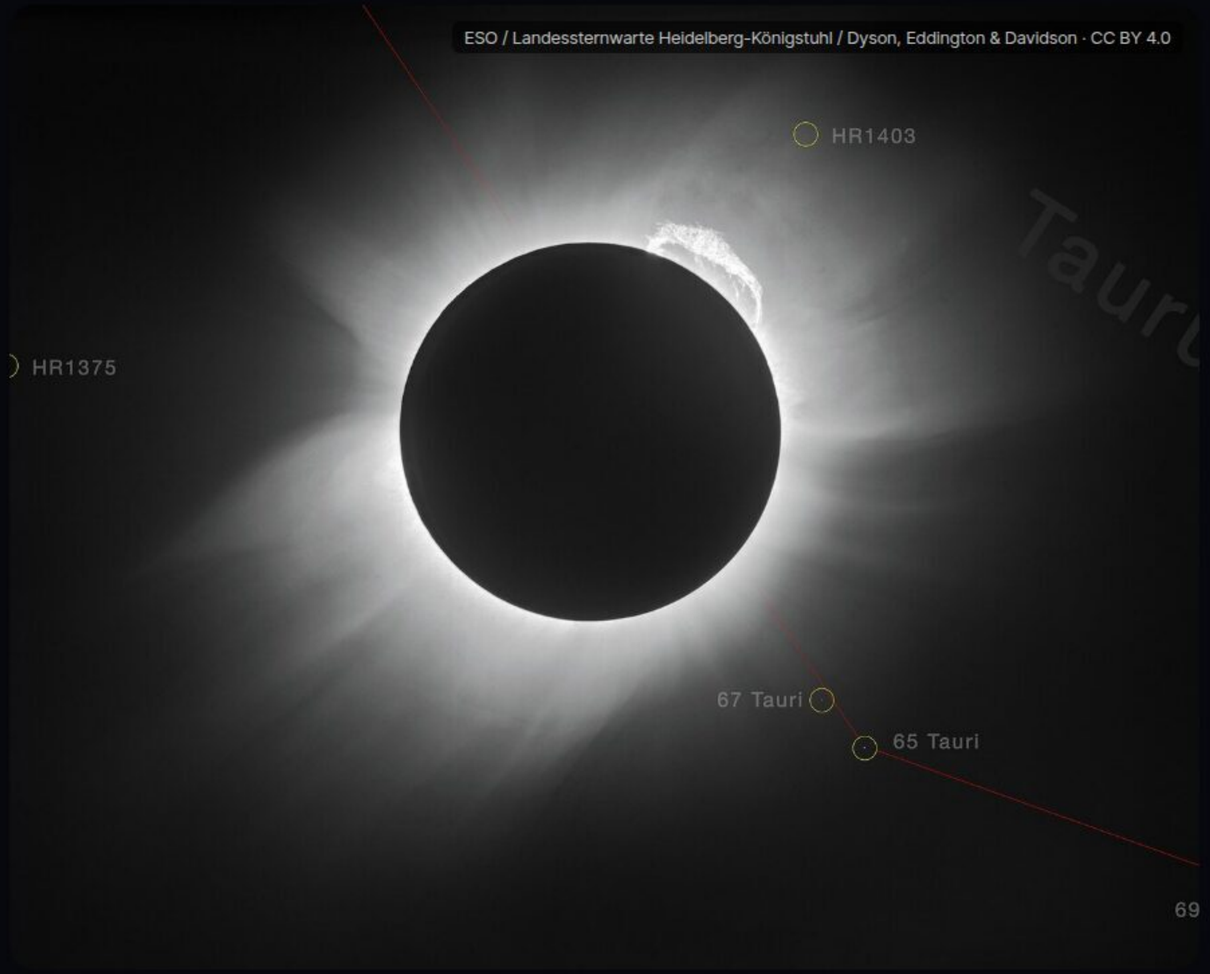
$$ds^2 = g_{\mu\nu} dx^\mu dx^\nu$$

THE METRIC IS THE FIELD

> *"Spacetime tells matter how to move; matter tells spacetime how to curve."*
>
> John A. Wheeler

THE CLASSICAL TESTS

Sobral, 1919: light *bends*



EFFECT	GR PREDICTS
perihelion of Mercury (1915)	43″ / century
light grazing the Sun (1919)	1.75″
redshift, Pound–Rebka (1959)	2.5×10^{-15} over 22.5 m
Shapiro delay (1964)	~200 µs
GPS clocks	+38 µs / day

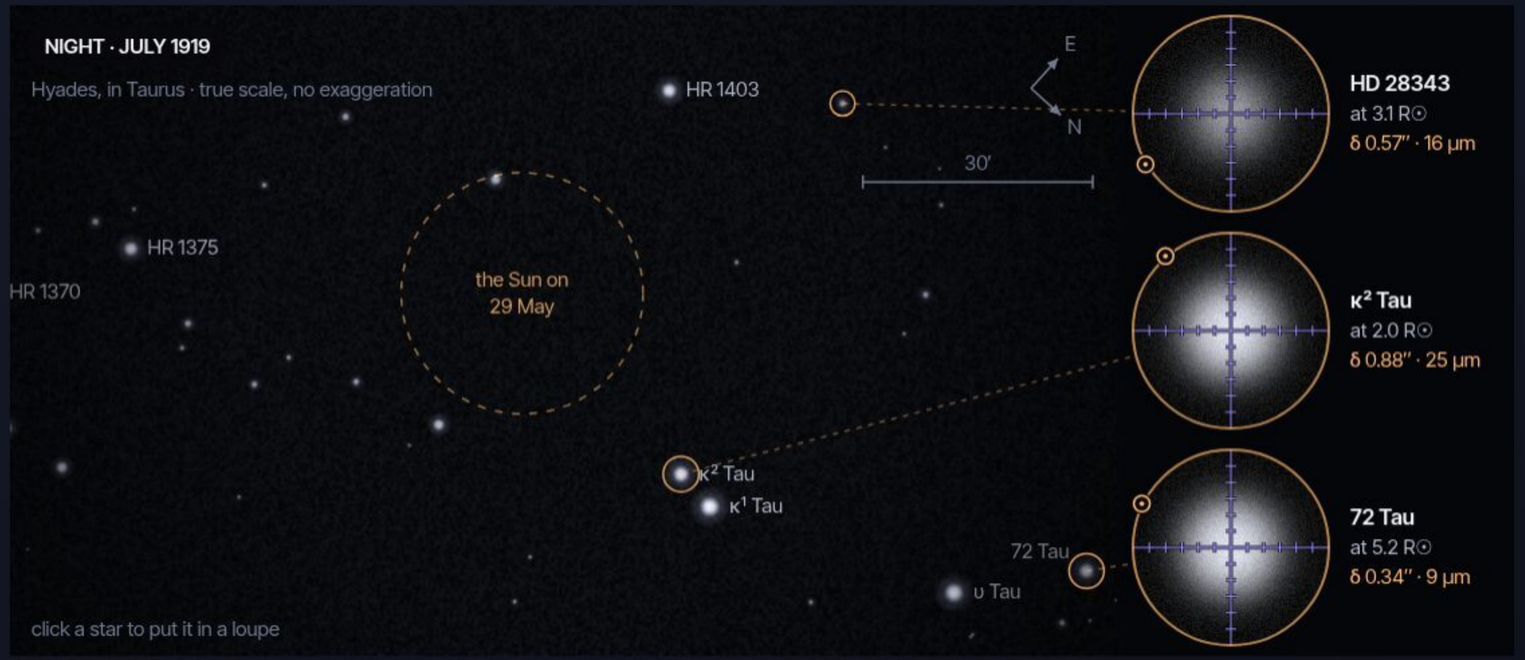
Sobral expedition (Ceará, Brazil): **1.98 ± 0.12″**. Príncipe: 1.61 ± 0.30″. The sky over north-eastern Brazil confirmed Einstein.

SOBRAL, 29 MAY 1919 · THE MEASUREMENT

Two plates, *the same sky*

SIMULATED PLATE · TRUE SCALE

blink | night | eclipse | both



width of the star image 2.0″

prediction: Einstein | Newton

on the 4-inch lens plate 1″ = 28 μm on screen 1″ = 0.10 px, in a loupe 24 px Sobral measured 1.98 ± 0.12″

Night: the Hyades photographed in July, before dawn, with the same telescope — the Sun far away.

Eclipse: the same field on 29 May, with the Moon covering the Sun. Every star moves away from the Sun, radially.

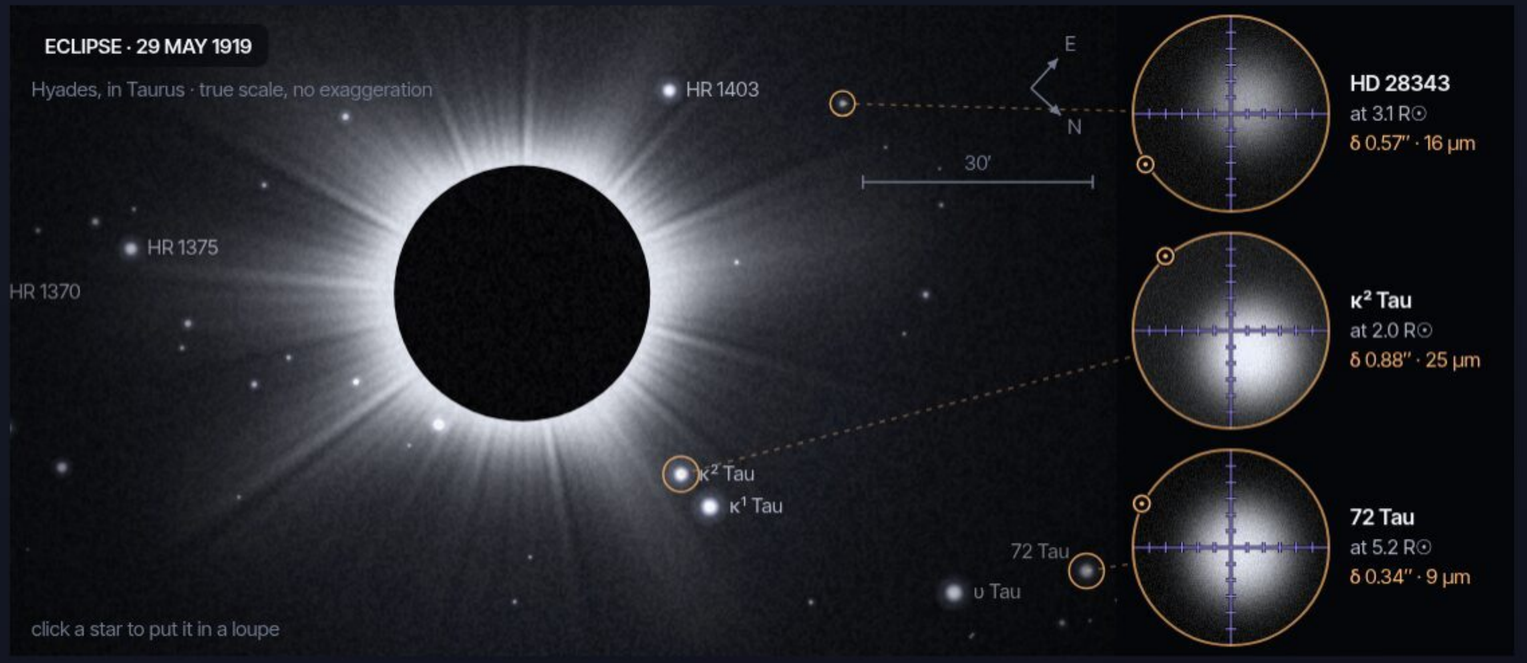
$$\delta = \frac{4GM}{c^2 b} = 1.75'' \frac{R_\odot}{b}$$

TWICE THE NEWTONIAN VALUE

On the whole plate nothing moves: 1″ is a tenth of a pixel. In the loupes, at true scale, as under the micrometer, the star jumps by a fraction of its own width — and the centre of a blob can be measured far better than its width.

SOBRAL, 29 MAY 1919 · THE MEASUREMENT

Two plates, *the same sky*



Night: the Hyades photographed in July, before dawn, with the same telescope — the Sun far away.

Eclipse: the same field on 29 May, with the Moon covering the Sun. Every star moves away from the Sun, radially.

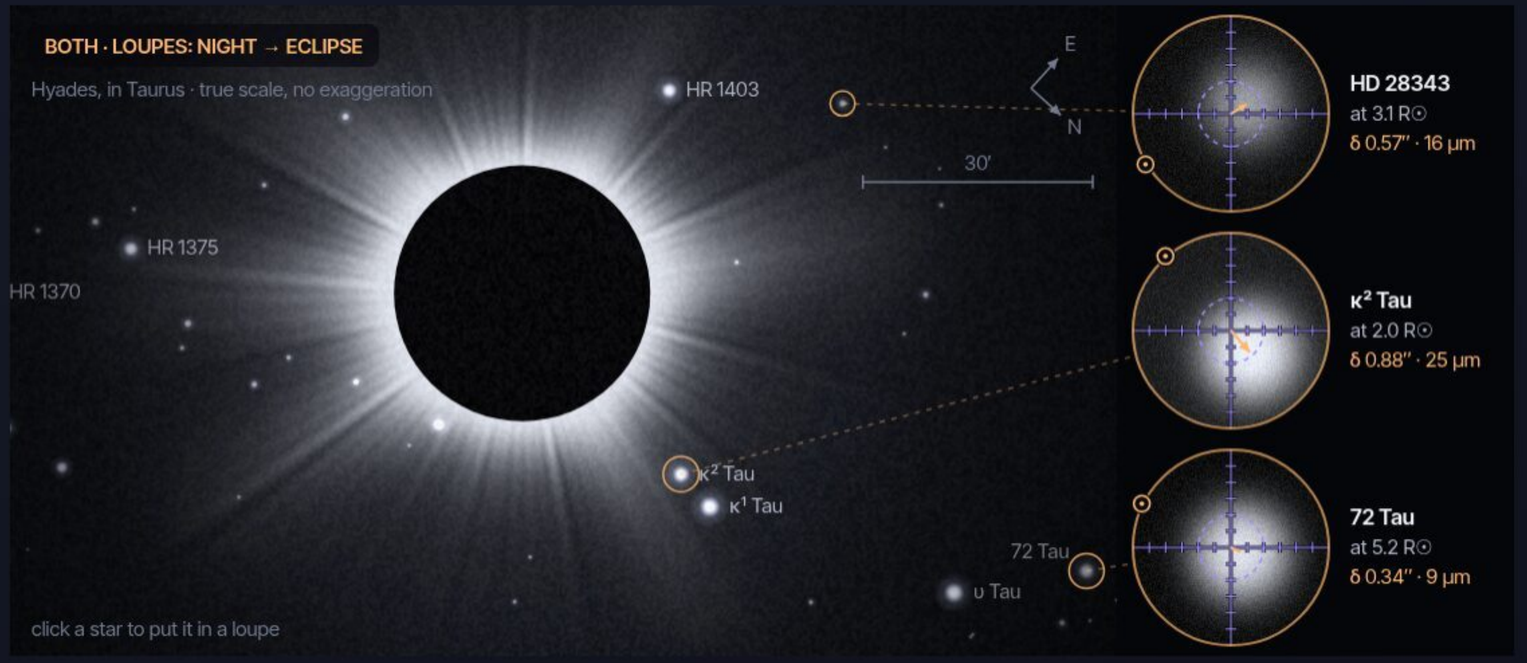
$$\delta = \frac{4GM}{c^2 b} = 1.75'' \frac{R_\odot}{b}$$

TWICE THE NEWTONIAN VALUE

On the whole plate nothing moves: 1″ is a tenth of a pixel. In the loupes, at true scale, as under the micrometer, the star jumps by a fraction of its own width — and the centre of a blob can be measured far better than its width.

SOBRAL, 29 MAY 1919 · THE MEASUREMENT

Two plates, *the same sky*



Night: the Hyades photographed in July, before dawn, with the same telescope — the Sun far away.

Eclipse: the same field on 29 May, with the Moon covering the Sun. Every star moves away from the Sun, radially.

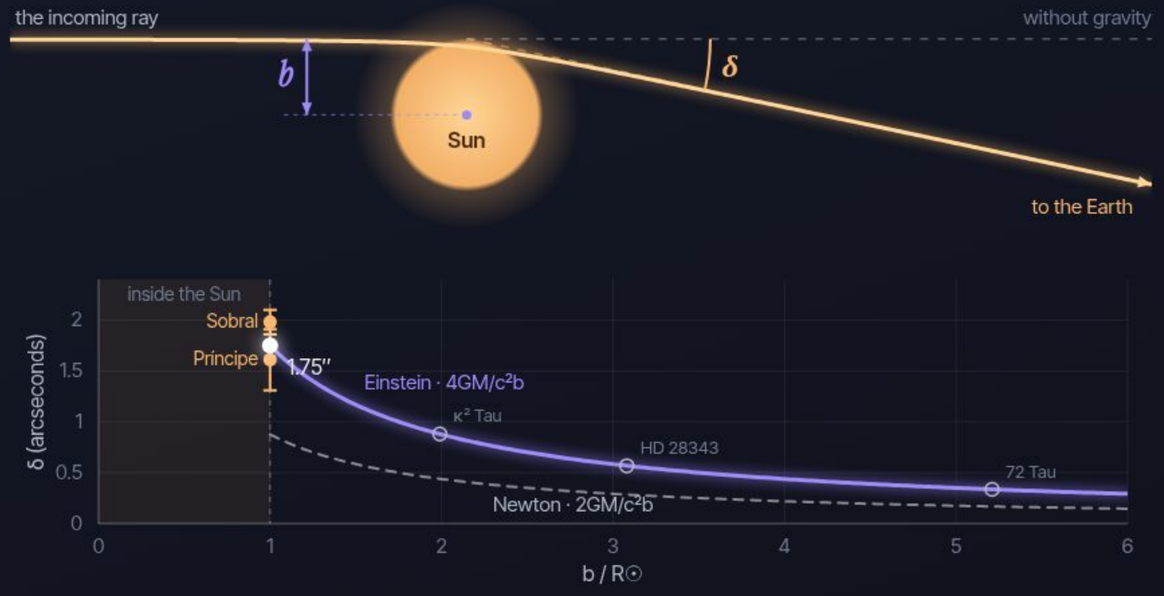
$$\delta = \frac{4GM}{c^2 b} = 1.75'' \frac{R_\odot}{b}$$

TWICE THE NEWTONIAN VALUE

On the whole plate nothing moves: 1″ is a tenth of a pixel. In the loupes, at true scale, as under the micrometer, the star jumps by a fraction of its own width — and the centre of a blob can be measured far better than its width.

Where *the 1.75″* comes from

deflection drawn 25,000× larger



impact parameter, $b/R_\odot$ 1.00

b 1.00 $R_\odot$ = 695,700 km δ 8.49×10^{-6} rad = 1.75″ Newton 0.88″

$$\delta = \frac{4GM_\odot}{c^2 b} = \frac{2r_s}{b}$$

b: FROM THE CENTRE OF THE SUN TO THE LINE OF THE INCOMING RAY

$$\left[\frac{GM}{c^2 b}\right] = \frac{(\mathrm{m^3\,kg^{-1}\,s^{-2}})(\mathrm{kg})}{(\mathrm{m^2\,s^{-2}})(\mathrm{m})} = 1$$

DIMENSIONLESS: THE ANGLE COMES OUT IN RADIANS

$$b = R_\odot:\ \delta = \frac{5.91\,\mathrm{km}}{6.96\times10^5\,\mathrm{km}} = 8.49\times10^{-6}\,\mathrm{rad}$$

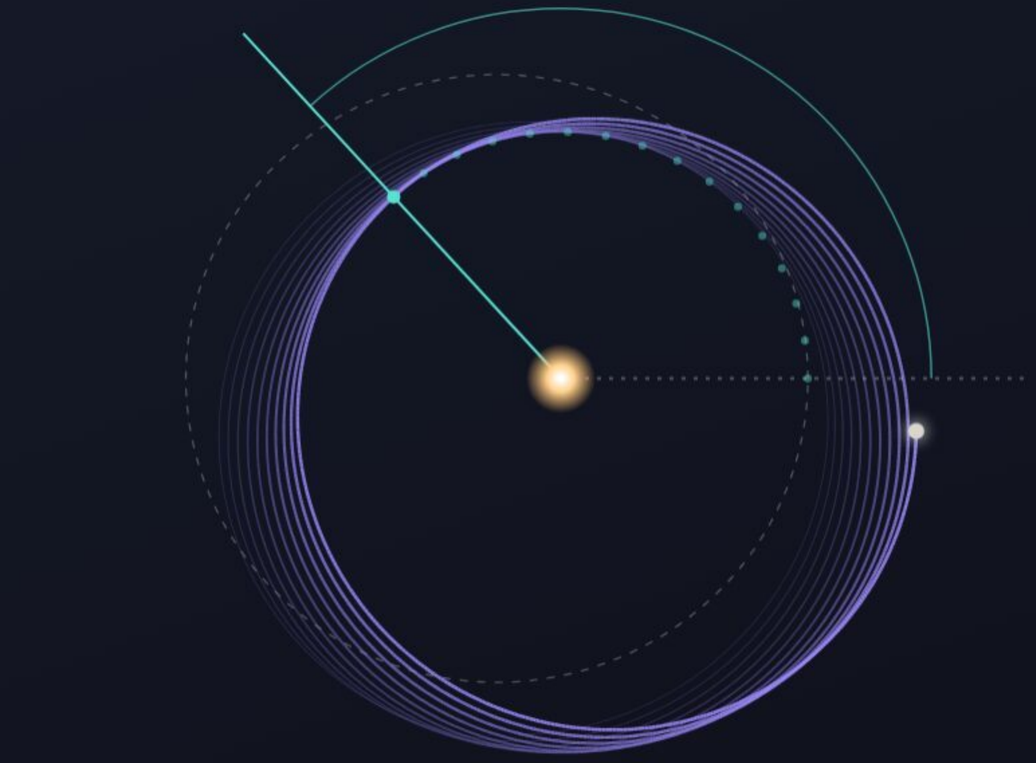
$4GM_\odot/c^2$ = 5.91 km: TWICE THE SUN'S r_s

$$1\,\mathrm{rad} = \frac{180}{\pi}\times 3600'' \approx 206{,}265'' \ \rightarrow\ \delta \approx 1.75''$$

NEWTON, WITH LIGHT AS A PARTICLE: HALF OF IT, 0.87″

1859 – 1915 · THE PERIHELION OF MERCURY

Mercury's orbit *does not close*



PERIHELION ADVANCE	PER CENTURY
observed (relative to the stars)	574″
other planets, by Newton	531″
unexplained remainder	43″

$$\Delta\varphi = \frac{6\pi G M_\odot}{c^2\, a(1-e^2)} = 0.104'' \text{ per orbit}$$

GR · EINSTEIN, NOVEMBER 1915 · 415 ORBITS PER CENTURY → 43.0″

Le Verrier found the remainder in 1859 and proposed a hidden planet, Vulcan. It was never found. Einstein got the 43″ with no adjustable parameter.

> *"For a few days, I was beside myself with joyous excitement."*
>
> Einstein to Ehrenfest, January 1916

DECEMBER 1915 · RUSSIAN FRONT

Schwarzschild and the *first exact solution*



Karl Schwarzschild
1873 – 1916

$$ds^2 = -\left(1 - \frac{r_s}{r}\right) c^2 dt^2 + \frac{dr^2}{1 - r_s/r} + r^2 d\Omega^2$$

$r_s = 2GM/c^2$ · VALID OUTSIDE ANY NON-ROTATING SPHERICAL BODY

$1\ r_s$	$1.5\ r_s$	$3\ r_s$	2.95 km
event horizon	photon sphere	ISCO: last stable orbit	r_s of the Sun (Earth: 8.9 mm)

He wrote to Einstein on 22 December 1915 while serving as an artillery officer. He died in May 1916.

WHAT WE NEED FROM THE METRIC

Curvature does *three things* to a photon

1 · IT BENDS THE PATH

The photon follows a **null geodesic**. Near the surface of a neutron star the bending is tens of degrees: we see **more than half** of the star.

2 · IT CHANGES THE ENERGY

A photon emitted at r with local energy E reaches infinity with

$$E_\infty = E\sqrt{(1 - R_S/r)}$$

GRAVITATIONAL REDSHIFT

3 · IT DELAYS

Different paths take different times (Shapiro delay): photons from each point of the star arrive tens of microseconds apart.

Ray tracing puts all three into a single calculation, **pixel by pixel**, for each instant of the rotation.

In a neutron star, $R \approx 2.5$–$3\ R_S$: none of the three effects is a small correction.

And all three depend only on the metric outside the star — which is why a light curve carries information about gravity.

Two constants *and a potential*

The metric depends on neither t nor ϕ: energy and angular momentum are conserved.

$$E = \left(1 - \frac{R_s}{r}\right)\dot{t}$$

$$L = r^2\,\dot{\varphi}$$

For light only the ratio matters, the **impact parameter** b = L/E:

$$\frac{1}{b^2} = \frac{\dot{r}^2}{L^2} + V(r), \quad V = \frac{1}{r^2}\left(1 - \frac{R_s}{r}\right)$$

A "POTENTIAL" FROM GEOMETRY ALONE

$$\left(\frac{du}{d\varphi}\right)^2 = \frac{1}{b^2} - u^2(1 - R_s u)$$

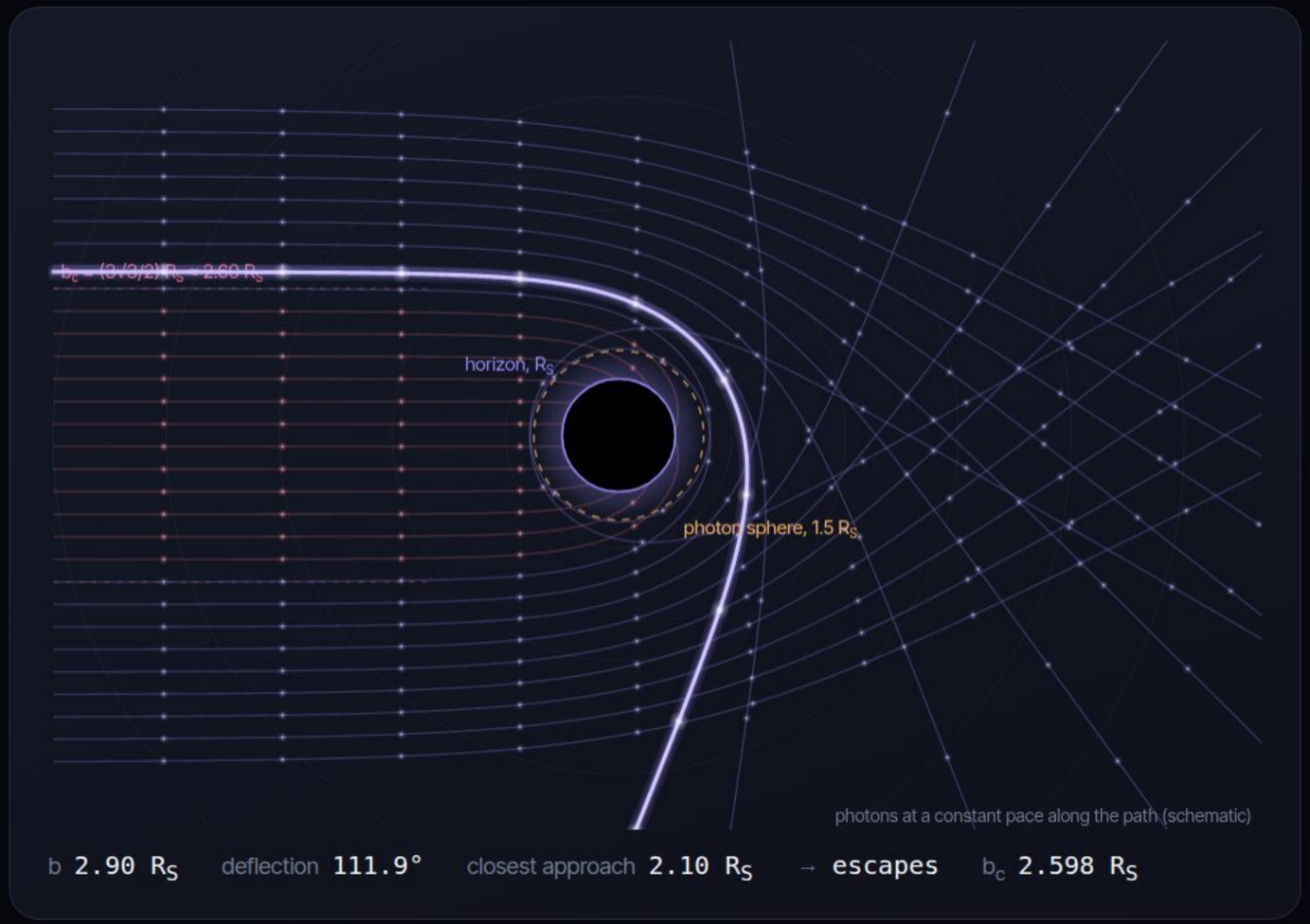
THE ORBIT · $u = 1/r$

The maximum of V lies at $r = 1.5\,R_S$: the **photon sphere**. Below $b_c = (3\sqrt{3}/2)\,R_S$ the ray comes from the horizon — or from the star.



SCHWARZSCHILD GEODESICS

How light *bends*



$$u'' + u = \frac{3}{2} R_S u^2$$

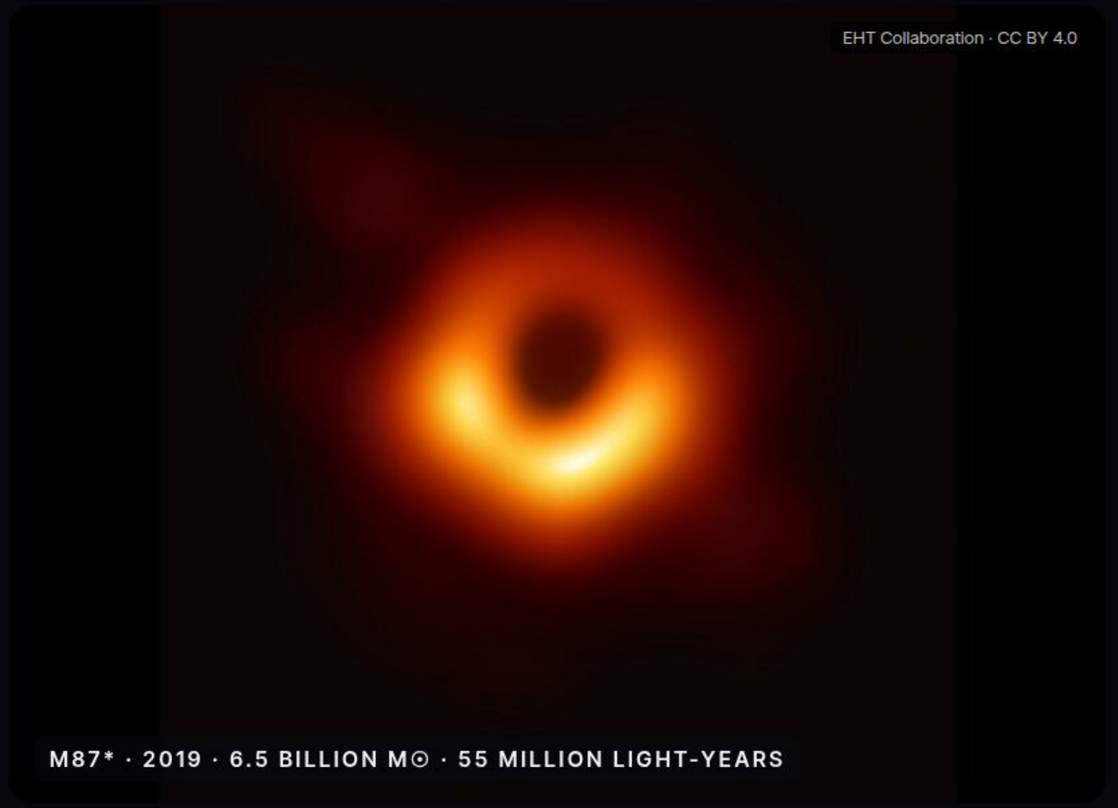
$u = 1/r$ · ORBIT EQUATION FOR LIGHT

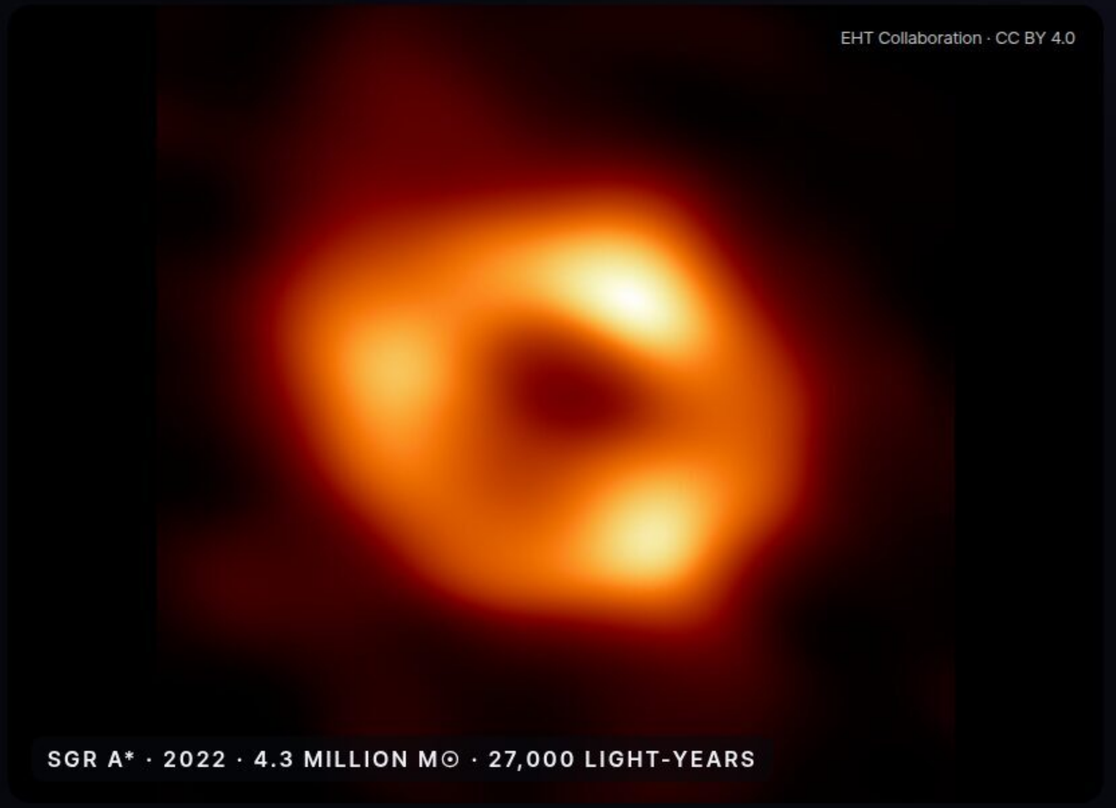
- $b > 3\sqrt{3}\,GM/c^2 \approx 2.6\ R_S$: the light is deflected and escapes.
- $b = 2.6\ R_S$: unstable orbit on the **photon sphere**, $r = 1.5\ R_S$.
- $b < 2.6\ R_S$: captured.

The term on the right is the General Relativity correction. Without it, light would travel in a straight line.

EVENT HORIZON TELESCOPE · 2019 AND 2022

The *shadows*





The ring is ~5 R_S across: it is the photon sphere, at 1.5 R_S, seen through the lens of the black hole itself — shadow diameter = $2\sqrt{27}\,GM/c^2 \approx 5.2\,R_S$.

COMPACTNESS

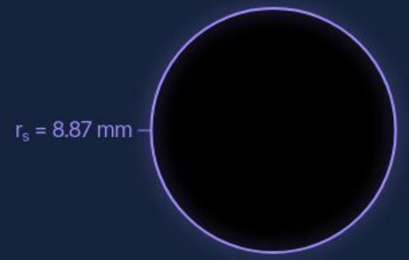
Where GR *stops being a correction*

• THE RADIUS AND THE SCHWARZSCHILD RADIUS OF THE SAME MASS

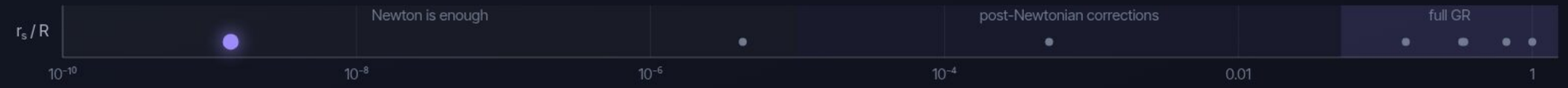
Earth | Sun | Sirius B | proto-NS | neutron star | ISCO | photon sph. | horizon

Earth — R = 6,371 km · the edge is off the frame

squeezed down to r_s, the Earth would be a black hole the size of a marble



mass · radius	5.97×10^{24} kg · 6,371 km
Schwarzschild radius, $r_s = 2GM/c^2$	8.87 mm
compactness, r_s/R	1.39×10^{-9}
escape velocity	11.2 km/s
surface gravity	1 g
redshift, z	6.96×10^{-10}
the surface clock loses	60.1 µs per day
grazing-ray deflection	5.7×10^{-4}″
surface seen from afar	50% + 7.0×10^{-8}%



Surface compared with infinity: $z = (1 - r_s/R)^{-1/2} - 1$, $g = (GM/R^2)(1 - r_s/R)^{-1/2}$ · deflection from the exact orbit integral (weak field: $2r_s/R$) · ISCO, photon sphere and horizon: a 1.4 M☉ star of that size · the objects advance on their own until the first click.

COMPACTNESS

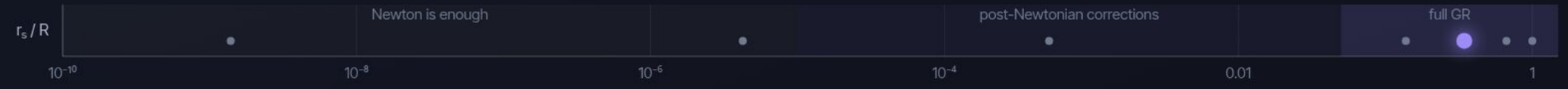
Where GR *stops being a correction*

• THE RADIUS AND THE SCHWARZSCHILD RADIUS OF THE SAME MASS

Earth | Sun | Sirius B | proto-NS | **neutron star** | ISCO | photon sph. | horizon



mass · radius	1.4 M⊙ · 12 km
Schwarzschild radius, $r_s = 2GM/c^2$	4.13 km
compactness, r_s/R	0.345
escape velocity	0.59 c
surface gravity	1.6×10^{11} g
redshift, z	0.235
the surface clock loses	4.57 h per day
grazing-ray deflection	61°
surface seen from afar	75.5%



Surface compared with infinity: $z = (1 - r_s/R)^{-1/2} - 1$, $g = (GM/R^2)(1 - r_s/R)^{-1/2}$ · deflection from the exact orbit integral (weak field: $2r_s/R$) · ISCO, photon sphere and horizon: a 1.4 M⊙ star of that size · the objects advance on their own until the first click.

THE ANGLE THAT MATTERS

From the surface to infinity: $\psi(\alpha)$

A photon leaves the surface at an angle α to the normal. By the time it reaches the observer, it has turned through ψ around the centre:

$$b = \frac{R \sin \alpha}{\sqrt{(1 - R_s/R)}}$$

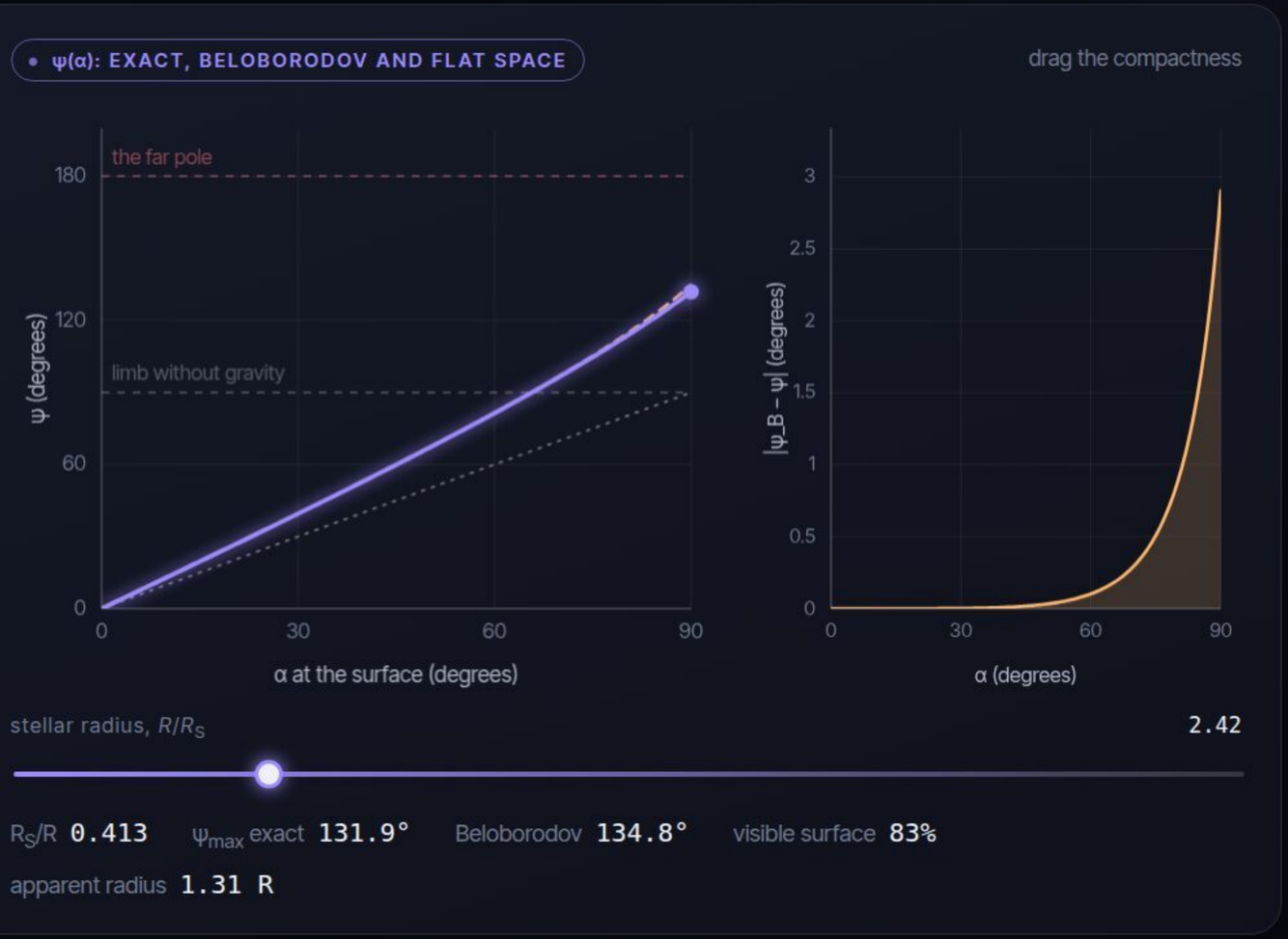
$$\psi(b) = \int_0^{1/R} \frac{du}{\sqrt{(b^{-2} - u^2(1 - R_s u))}}$$

EXACT

$$1 - \cos \alpha \approx (1 - \cos \psi)(1 - \frac{R_s}{R})$$

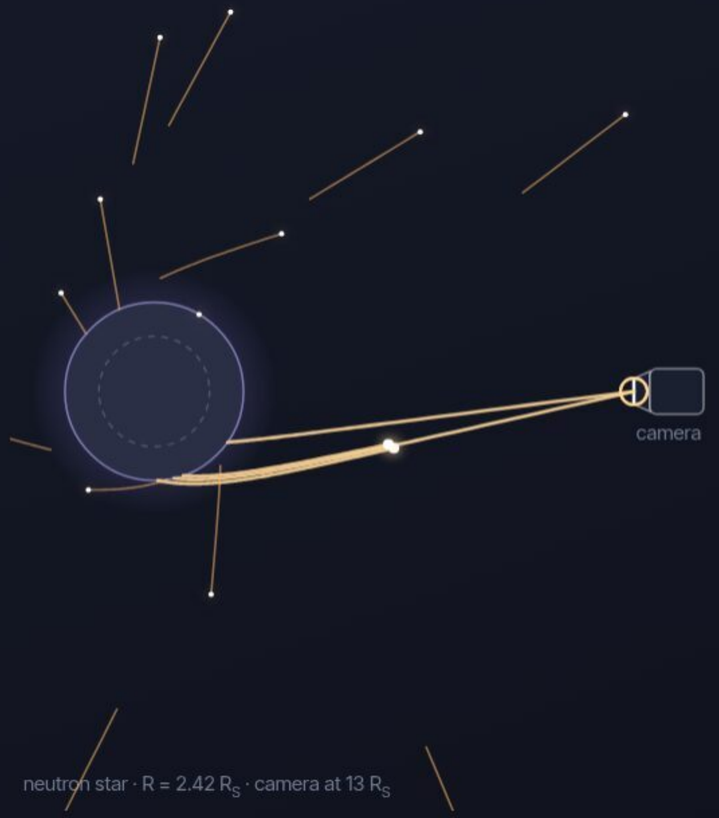
BELOBORODOV (2002)

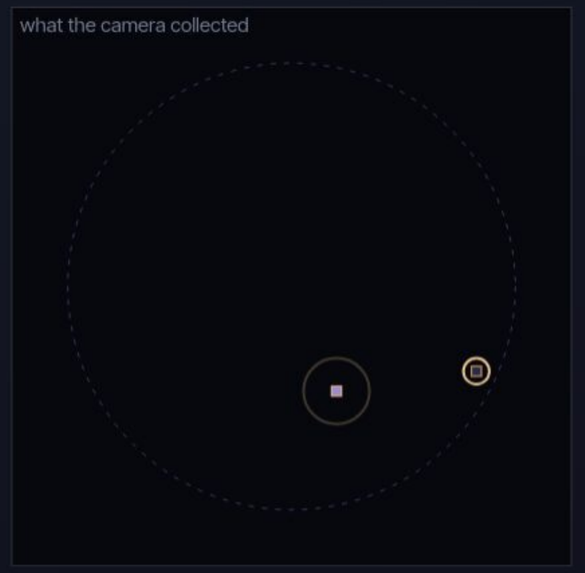
Without gravity, ψ = α and the limb is at 90°. With gravity, the limb moves further round: **we see behind the star**. The approximation is excellent down to $R \approx 3\ R_S$ and fails precisely where the secondary image appears.



THE NAIVE IDEA: FROM THE STAR TO THE CAMERA

Many rays, *hardly any pixels*





neutron star · R = 2.42 R_S · camera at 13 R_S

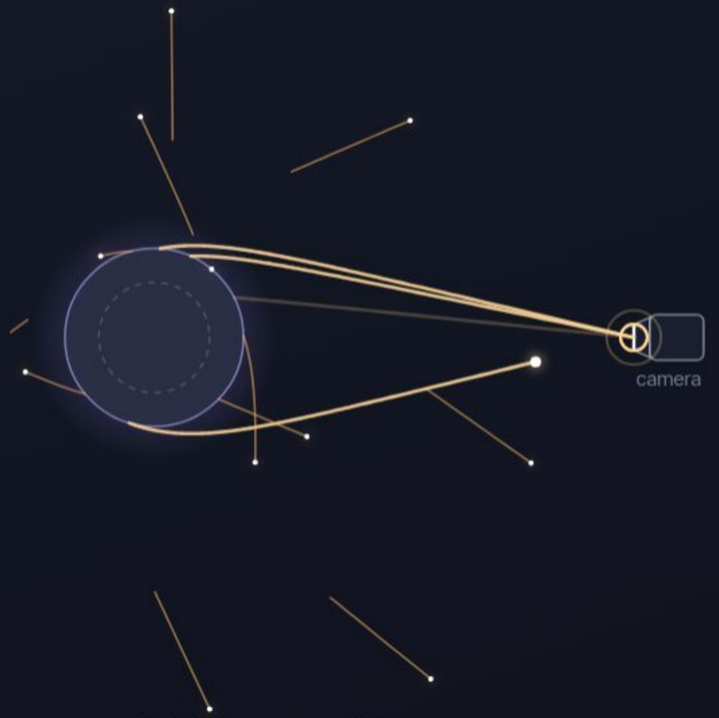
rays launched **10,400** entered the camera **4** (0.038%) pixels lit **2** of 1,568 full image in **~5 h**

- Every point of the surface emits in **every direction**; each ray is followed along its geodesic, outwards.
- Only those that pass through the camera aperture become pixels: here, **2 in every 10,000**.
- Completing this image would take ~10^8 rays: hours of computing.
- With a real telescope, 1 m^2 at 1 kpc, **1 photon in every 10^{40}** arrives.

3D count: uniform point on the surface, isotropic outward direction, exact geodesic to the camera, at 13 R_S. Only a sample is drawn, in the plane; the rays that enter the camera are all shown.

THE NAIVE IDEA: FROM THE STAR TO THE CAMERA

Many rays, *hardly any pixels*



neutron star · R = 2.42 R_S · camera at 13 R_S



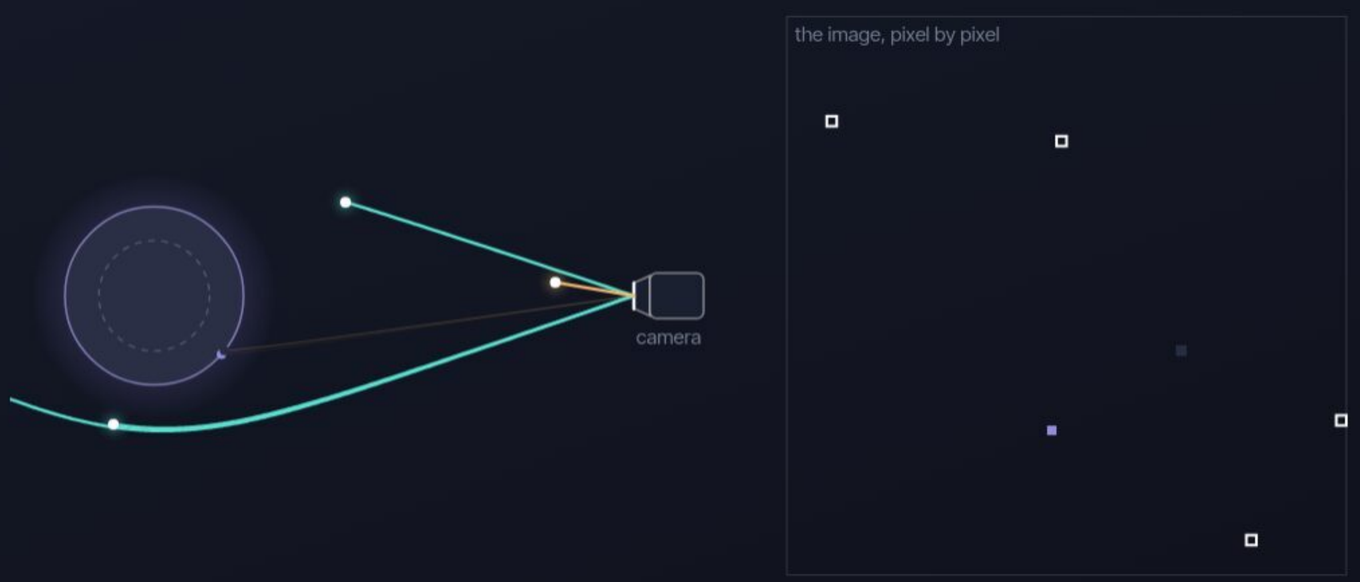
rays launched **180,000** entered the camera **34** (0.019%) pixels lit **31** of 1,568 full image in **~5 h**

- Every point of the surface emits in **every direction**; each ray is followed along its geodesic, outwards.
- Only those that pass through the camera aperture become pixels: here, **2 in every 10,000**.
- Completing this image would take ~10^8 rays: hours of computing.
- With a real telescope, 1 m^2 at 1 kpc, **1 photon in every 10^{40}** arrives.

3D count: uniform point on the surface, isotropic outward direction, exact geodesic to the camera, at 13 R_S. Only a sample is drawn, in the plane; the rays that enter the camera are all shown.

THE METHOD: FROM THE CAMERA TO THE STAR

One pixel, *one ray*



neutron star · R = 2.42 R_S · camera at 13 R_S

pixel (27, 12) · θ 9.3° · b 2.20 R_S hits the surface · α 44° · ψ 49° rays computed = pixels 6 (0%)

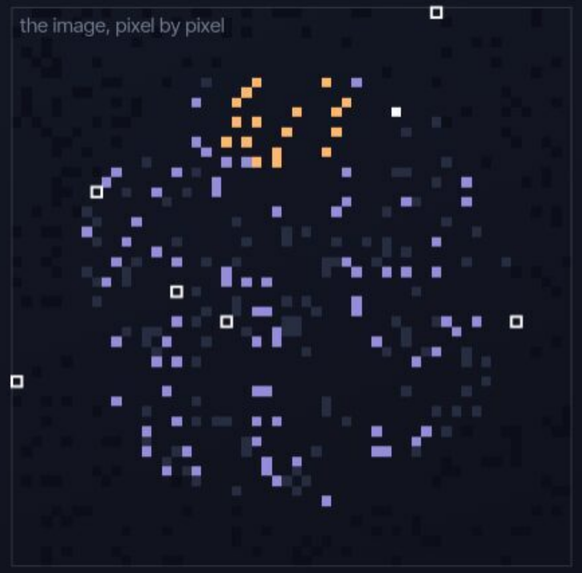
- The rays leave the **camera**, one per pixel: the path of light travelled backwards. The direction of the pixel gives the impact parameter *b*.
- The geodesic is integrated until the ray escapes to the sky or hits the surface at some point, at an angle α.
- The pixel takes the colour of the point the light left from — corrected for redshift and for the emission angle.
- Every ray computed becomes a pixel: **3,136 rays, 3,136 pixels**, against the 10^8 of the previous slide.

With spherical symmetry, ψ depends only on *b*: one table ψ(*b*), computed once, serves every pixel. Each ray is rotated into the plane of the drawing.

THE METHOD: FROM THE CAMERA TO THE STAR

One pixel, *one ray*





neutron star · R = 2.42 R_S · camera at 13 R_S

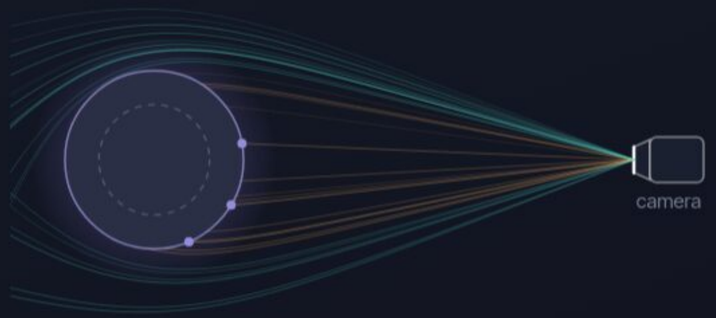
pixel (21, 31) · θ 4.4° · b 1.05 R_S hits the surface · α 19° · ψ 21° rays computed = pixels 409 (13%)

- The rays leave the **camera**, one per pixel: the path of light travelled backwards. The direction of the pixel gives the impact parameter *b*.
- The geodesic is integrated until the ray escapes to the sky or hits the surface at some point, at an angle α.
- The pixel takes the colour of the point the light left from — corrected for redshift and for the emission angle.
- Every ray computed becomes a pixel: **3,136 rays, 3,136 pixels**, against the 10^8 of the previous slide.

With spherical symmetry, ψ depends only on *b*: one table ψ(*b*), computed once, serves every pixel. Each ray is rotated into the plane of the drawing.

THE METHOD: FROM THE CAMERA TO THE STAR

One pixel, *one ray*





neutron star · R = 2.42 R_S · camera at 13 R_S

pixel (34, 3) · θ 15.3° · b 3.57 R_S escapes: sky rays computed = pixels 3,136 (100%)

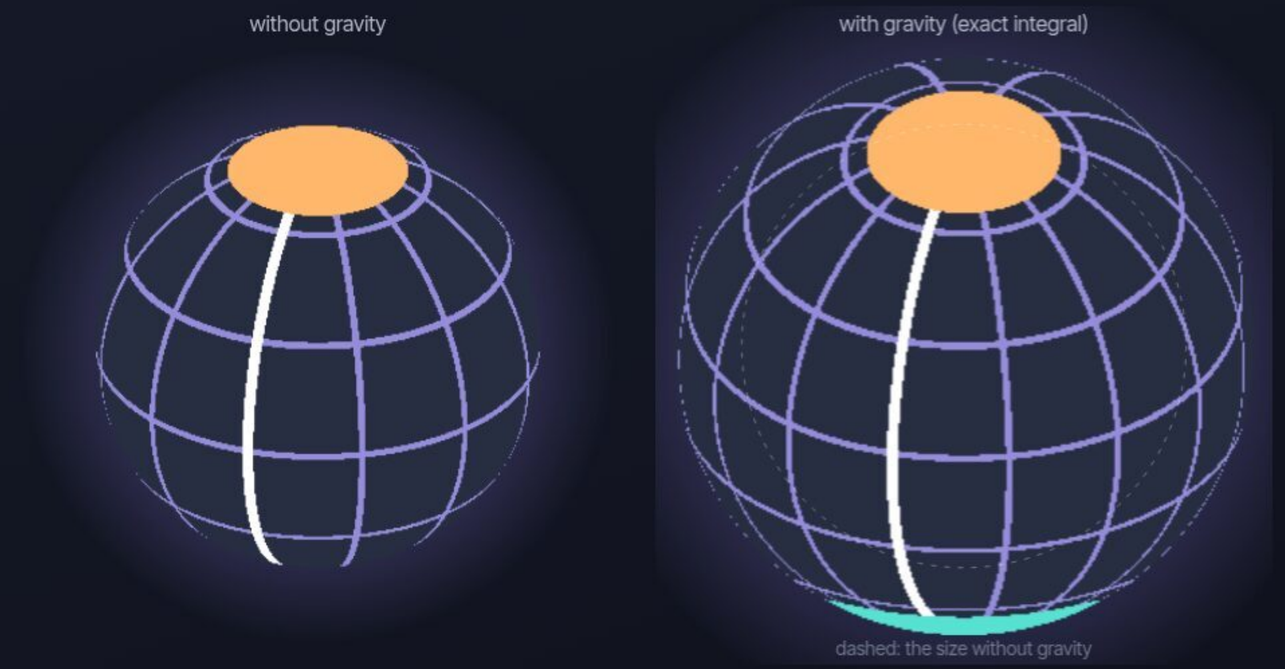
- The rays leave the **camera**, one per pixel: the path of light travelled backwards. The direction of the pixel gives the impact parameter ***b***.
- The geodesic is integrated until the ray escapes to the sky or hits the surface at some point, at an angle α.
- The pixel takes the colour of the point the light left from — corrected for redshift and for the emission angle.
- Every ray computed becomes a pixel: **3,136 rays, 3,136 pixels**, against the 10^8 of the previous slide.

With spherical symmetry, ψ depends only on ***b***: one table ψ(***b***), computed once, serves every pixel. Each ray is rotated into the plane of the drawing.

We see *behind* the star

THE SAME STAR, MORE AND MORE COMPACT · EXACT INTEGRAL

drag the compactness and the inclination



radius, R/R_S 2.42

axis inclination 60°

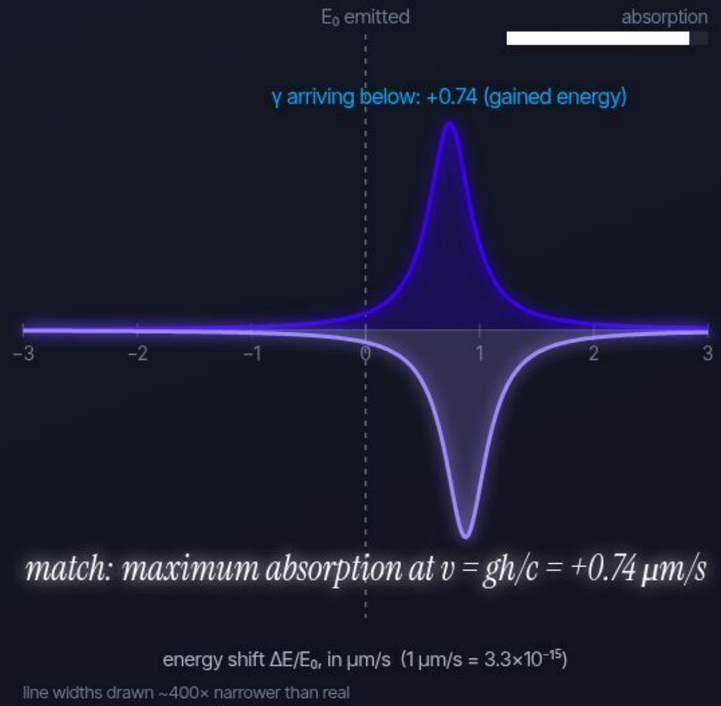
R 2.42 R_S ψ_{max} 131.9° visible surface 83% (without gravity: 50%) apparent radius 1.31×

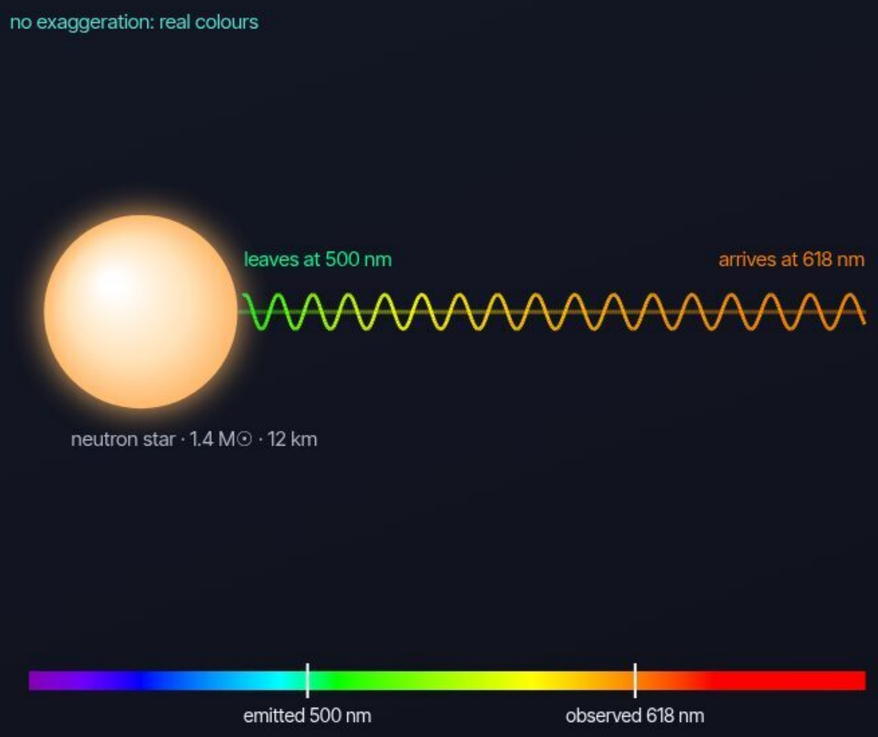
On the left, the star as it would look without gravity; on the right, ray-traced. The grid is the same; gravity bends the light around the star and reveals the **far hemisphere**.

- The image is larger: apparent radius $R/\sqrt{(1 - R_S/R)}$.
- For $R < 1.76\ R_S$ the whole surface is visible — the far pole becomes a ring.
- Below $1.5\ R_S$ the star would lie inside the photon sphere.

Light *loses energy as it climbs*







tower $\Delta\nu/\nu = gh/c^2$ **2.46×10⁻¹⁵** resonance at **+0,74 μm/s** ≈ 2.7 mm per hour absorber now **0.88 μm/s** star $1 + z = (1 - r_s/R)^{-½}$ **1.235**

14.4 keV γ rays from ⁵⁷Fe (Mössbauer effect). Pound & Rebka, PRL 4, 337 (1960): ~10%; Pound & Snider, Phys. Rev. 140, B788 (1965): ~1%. Every 12 s source and absorber swap places, as in the experiment.

The spectrum that *climbs out of the well*

Along a ray, I_ν/ν^3 is conserved. With $g = \sqrt{(1 - R_S/R)}$:

$$I_{obs}(E) = g^3 I_{em}(E/g)$$

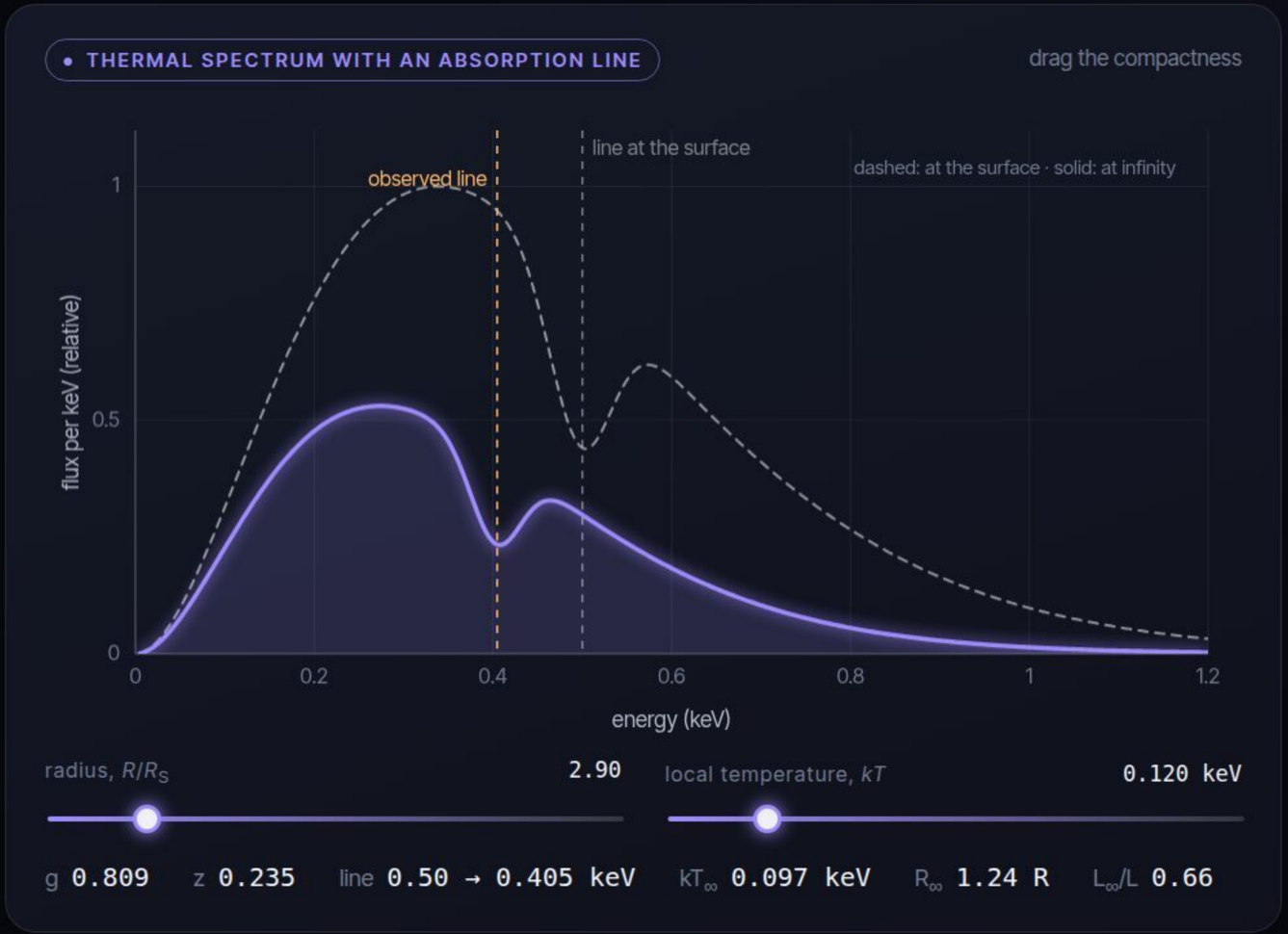
SPECIFIC INTENSITY

$T_\infty = g\,T$

$R_\infty = R/g$

A black body stays a black body, only cooler. The luminosity seen from afar is $L_\infty = g^2\,L$.

A **spectral line** of known energy E_0 arrives at $g\,E_0$: measuring the line means measuring the **compactness**.



PART II IN SUMMARY

The *ray tracing* recipe

1. **Choose the exterior metric**: Schwarzschild; Hartle–Thorne or Kerr with rotation; a different one for a different theory of gravity.
2. **Build the table** $\psi(b)$ and the delay $\Delta t(b)$ by integrating the null geodesics once.
3. **For each pixel** (or each surface element): $b \to$ emitting point, angle α, redshift g, delay.
4. **Intensity**: $I_{obs} = g^3\, I(E/g, \alpha')$, with the atmosphere's beaming and the Doppler shift from rotation.
5. **Add up**: image, flux — and, phase by phase, the **light curve** and the phase-resolved spectrum.

EXACT OR APPROXIMATE?

- **Exact integral** (or elliptic integrals): always valid, secondary images included.
- **Beloborodov (2002)** and Poutanen & Beloborodov (2006): closed formulae for ψ and for the delay, excellent for $R \gtrsim 3\ R_S$.
- **Oblate Schwarzschild** (Morsink et al. 2007): a star flattened by rotation, for millisecond pulsars.

This is the engine behind NICER's mass and radius measurements — and behind the results of Part IV.

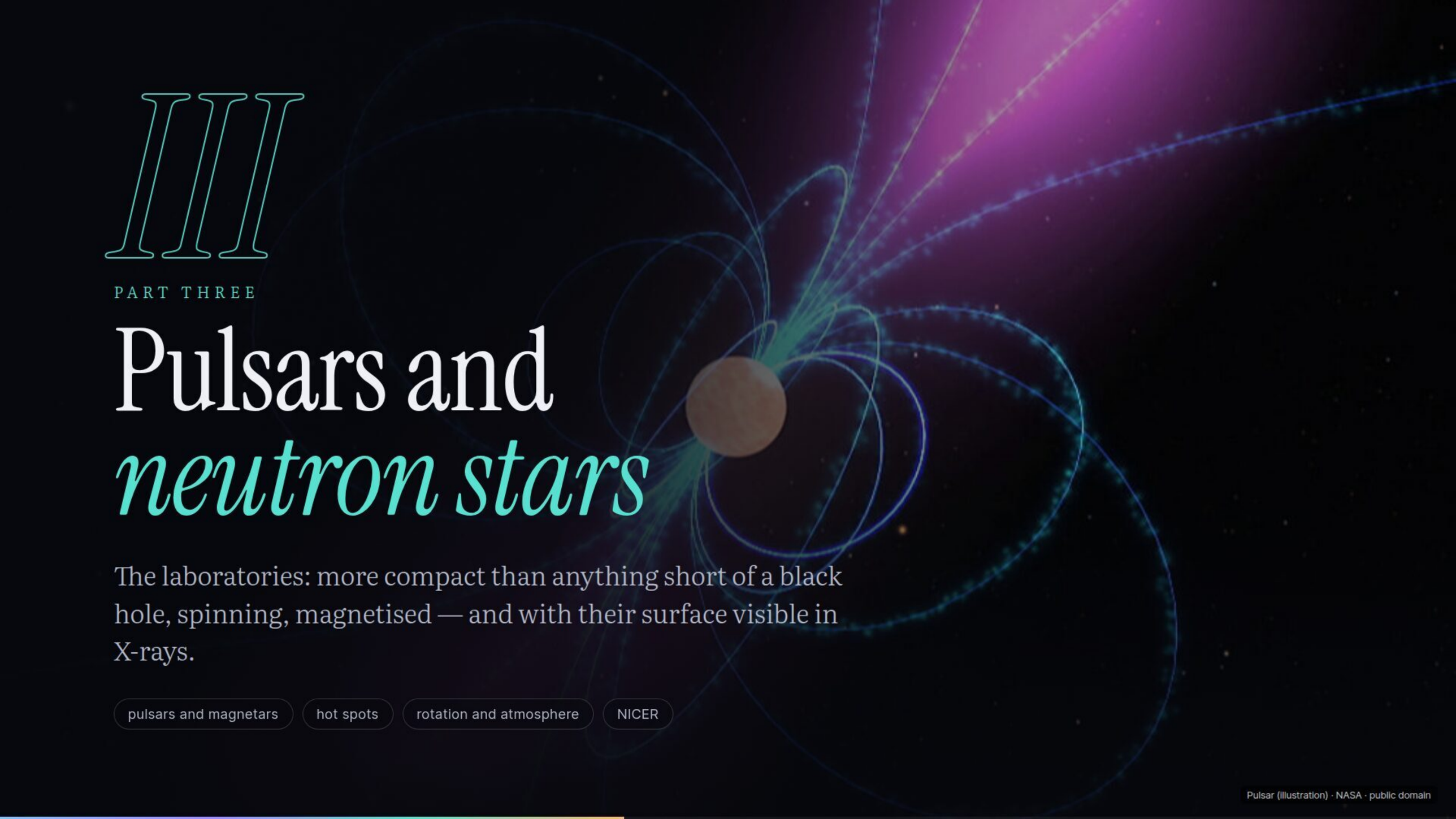
III

PART THREE

Pulsars and *neutron stars*

The laboratories: more compact than anything short of a black hole, spinning, magnetised — and with their surface visible in X-rays.

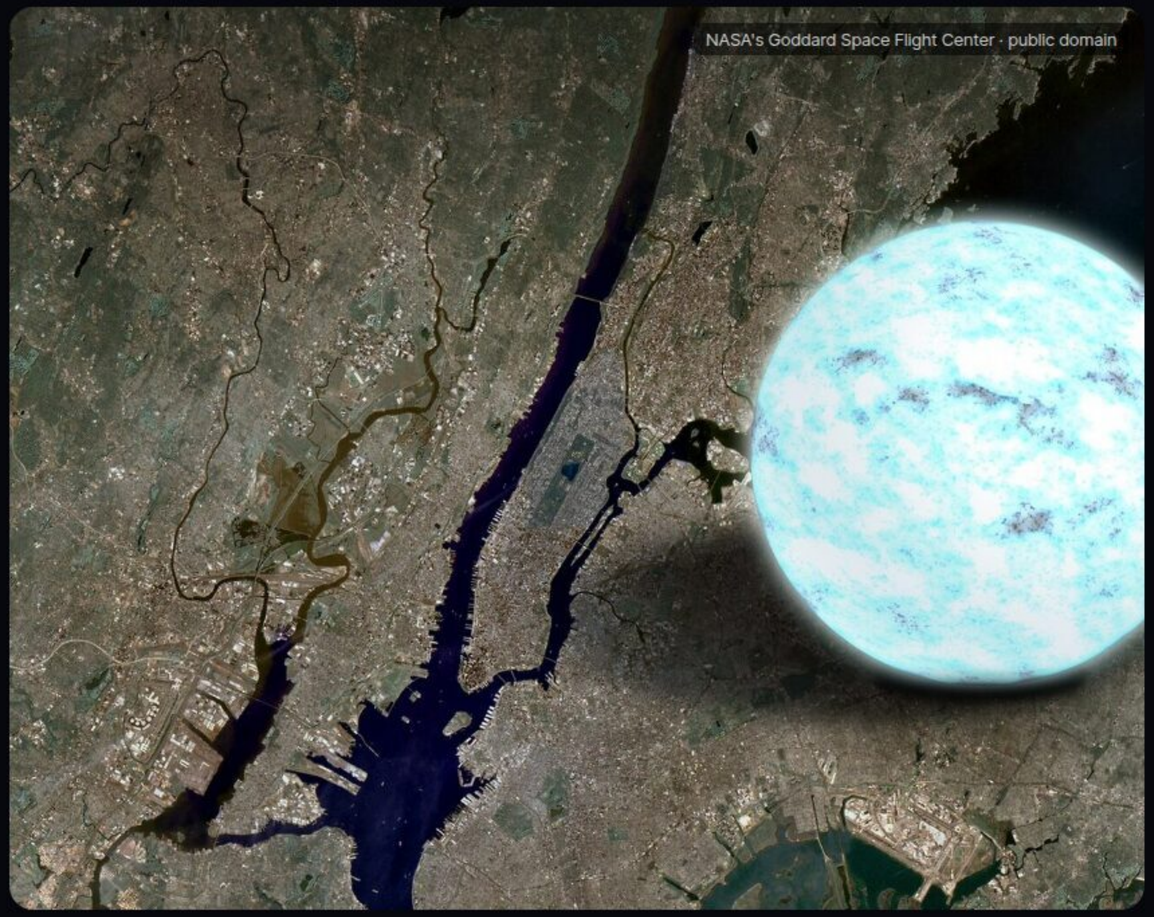
pulsars and magnetars | hot spots | rotation and atmosphere | NICER



Pulsar (illustration) · NASA · public domain

NEUTRON STARS IN NUMBERS

A solar mass *in a city*



A neutron star ~20 km across over Manhattan, to scale.

1.1–2.1 $M_\odot$
measured masses

11–13 km
radius (NICER, gravitational waves)

2–3 R_S
compactness: the regime of Part II

10^8–10^{15} G
surface magnetic field

Central density a few times that of the atomic nucleus, ~10^{15} g/cm^3. Spin periods from **1.4 ms** to tens of seconds.

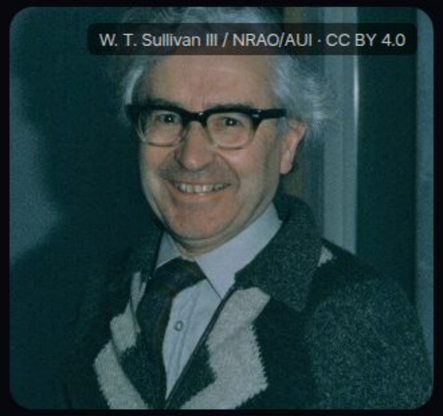
Surface gravity is ~10^{11} times the Earth's; the escape velocity, 0.5 to 0.7 **c**.

CAMBRIDGE · 28 NOVEMBER 1967

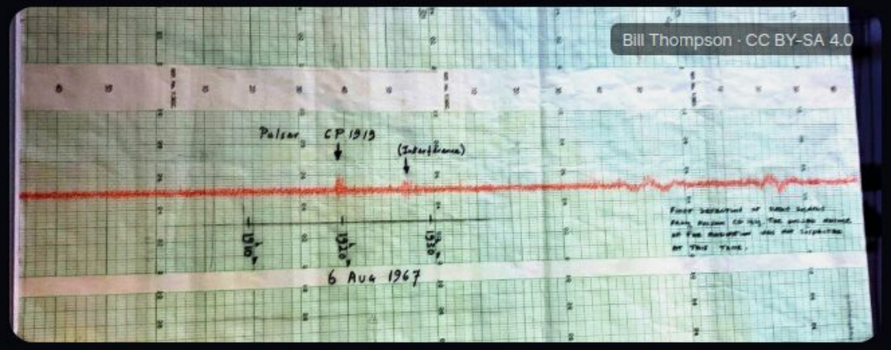
The first pulsar: *"LGM-1"*



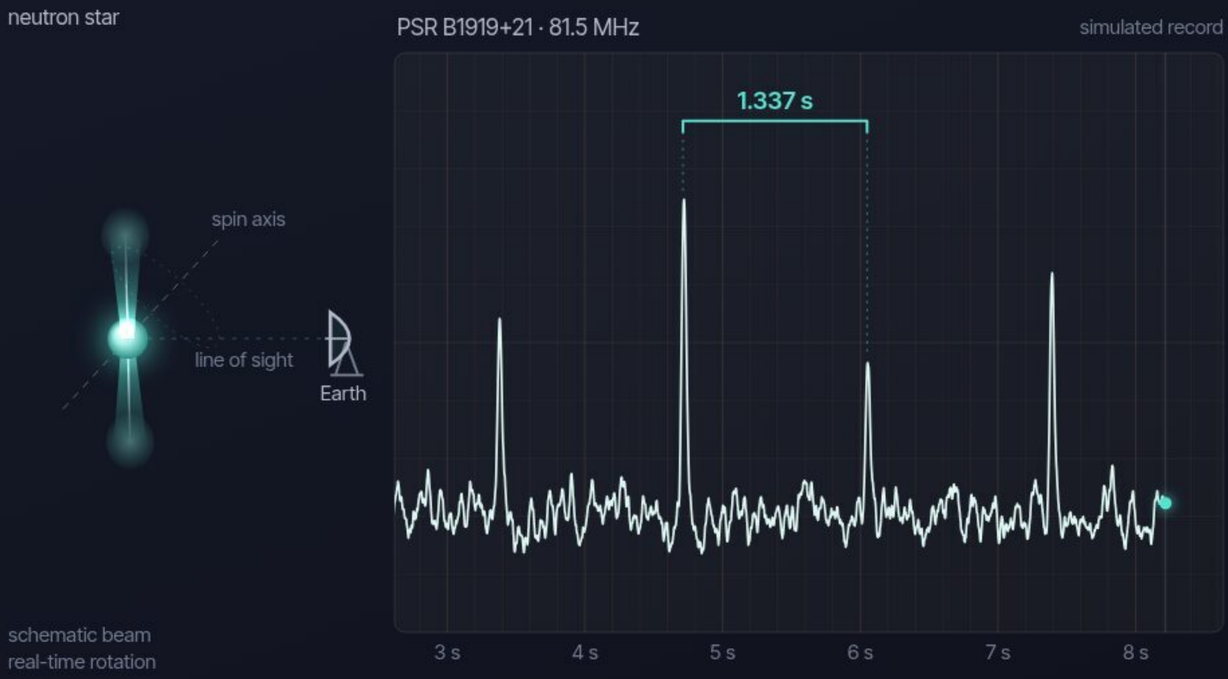
Jocelyn Bell
in 1967, PhD student



Antony Hewish
supervisor · Nobel Prize 1974



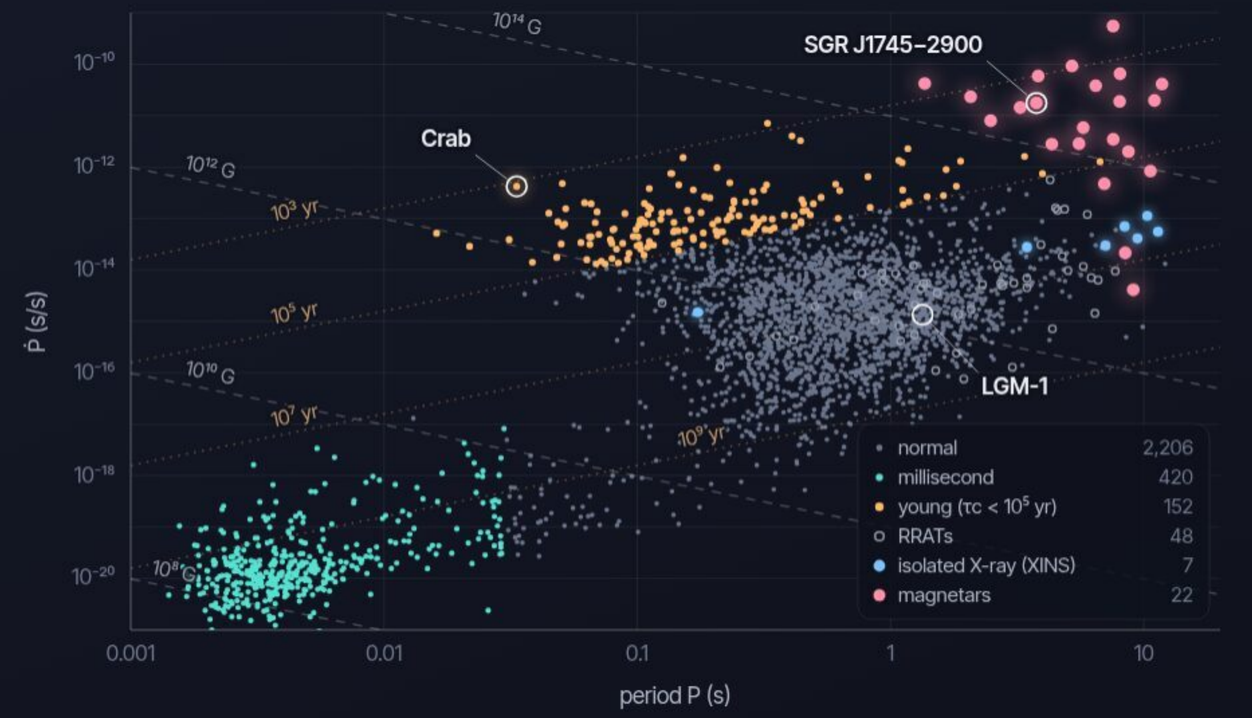
The original chart, August 1967: the "scruff" pencilled in as CP 1919.



period **1.337 302 s** $\dot{P}$ **1.35×10^{-15} s/s** frequency **81.5 MHz** pulses recorded **6**

Bell noticed a bit of "scruff" that kept coming back on the radio telescope's paper chart: pulses every **1.337 s**, as regular as clockwork. Nickname: **LGM-1**, for *Little Green Men*. It was a spinning neutron star.

What is measured, *and what is inferred*



OBSERVABLE	EXPRESSION
period	P
characteristic age	$t_c = P/2\dot{P}$
magnetic field	$B = (3Ic^3P\dot{P}/8\pi^2R^6)^{1/2}$
rotational energy lost	$\dot{E}_{rot} = -4\pi^2I\dot{P}/P^3$

CANONICAL NEUTRON STAR

$M = 1.4\ M_\odot \cdot R = 10\ km \cdot I = 10^{45}\ g\ cm^2$

$B = 3.2\times10^{19}\ (P\dot{P})^{1/2}\ G$

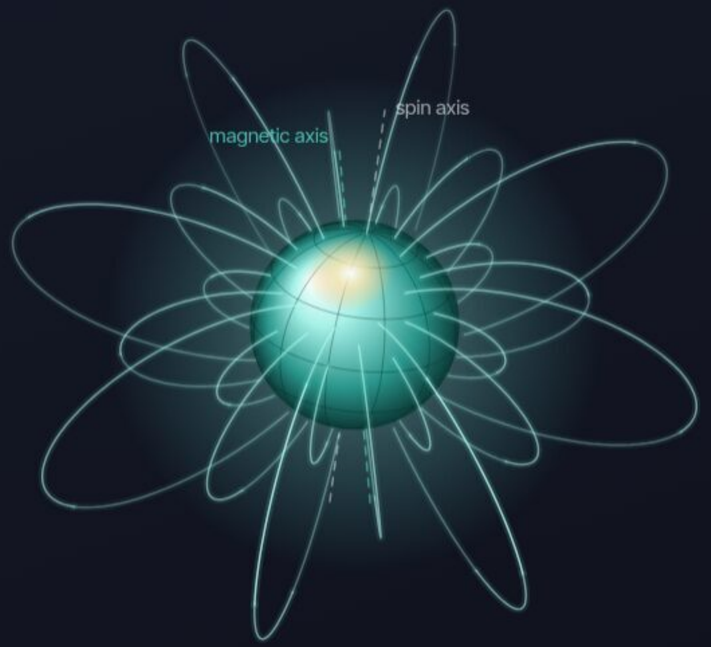
$|\dot{E}_{rot}| = 3.9\times10^{46}\ \dot{P}/P^3\ erg/s$

Only P and $\dot{P}$ are measured. The rest comes from assuming a spinning magnetic dipole — the straight lines in the diagram.

TRANSIENT ACTIVITY

A magnetar, *spinning*

SGR J1745−2900



field lines of a tilted dipole · real-time rotation

illustrative bursts

P 3.76 s B ≈ 2.6×10¹⁴ G characteristic age ≈ 3,400 yr $\dot{E}_{rot}$ ≈ 1.3×10³⁴ erg/s

bursts seen 1

EVENT	ENERGY
short bursts (~0.1 s)	10^{39} – 10^{41} erg
outbursts (months)	10^{41} – 10^{43} erg
giant flares	10^{44} – 10^{46} erg

The field lines, anchored in the crust, get twisted over time. When the crust can no longer take the stress, it cracks — a **starquake** — and the magnetic energy comes out all at once.

Giant flares in the Galaxy and the Magellanic Clouds: 1979, 1998 and 2004.

Why *hot spots* appear

MILLISECOND PULSARS

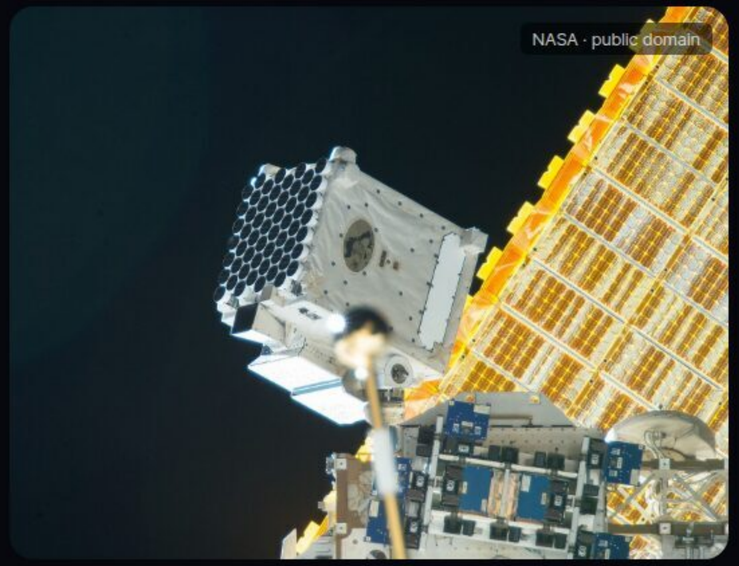
Particles accelerated in the magnetosphere flow back and **heat the polar caps** to ~10^6 K. They are NICER's targets.

MAGNETARS

Field decay and the currents along twisted field lines heat regions of the crust — which change after each *outburst*.

ISOLATED COOLING STARS

The magnetic field makes **heat conduction anisotropic**: poles hotter than the equator (the "Magnificent Seven").



NICER · on the Space Station since 2017 · ~100 ns time resolution



XMM-Newton · ESA, since 1999 · the largest area in soft X-rays



Chandra · NASA, since 1999 · the sharpest angular resolution

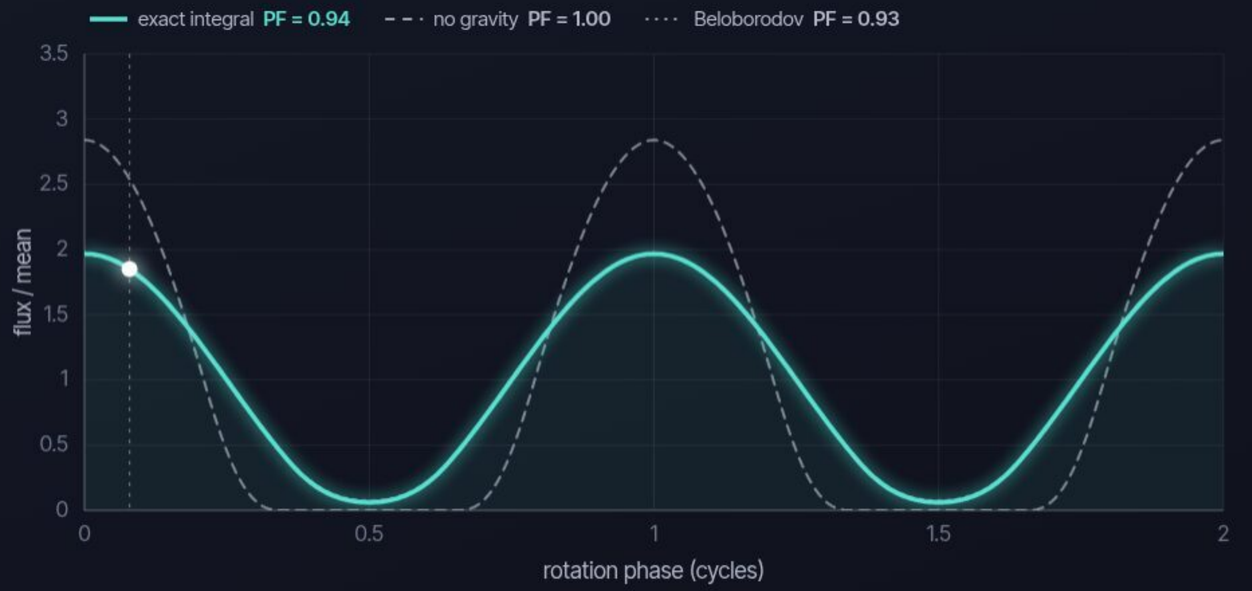
One spot, *one light curve*

• STATIC STAR · EXACT INTEGRAL, BELOBORODOV OR FLAT SPACE

no gravity | Beloborodov | exact integral



static star · 1 turn per 4 s
sizes in units of R



radius, R/R_S 2.42 | spot ↔ axis, i 60° | observer ↔ axis, j 75° | angular radius of the spot 20°

PF no gravity `1.000` PF Beloborodov `0.928` PF exact `0.939` surface visible `83%` ψ_{max} `131.9°` class `B · centre hidden 10% of the turn (the rim stays)`

secondary image `no (needs R < 1.76 R_S)`

Antipodal, *or not*

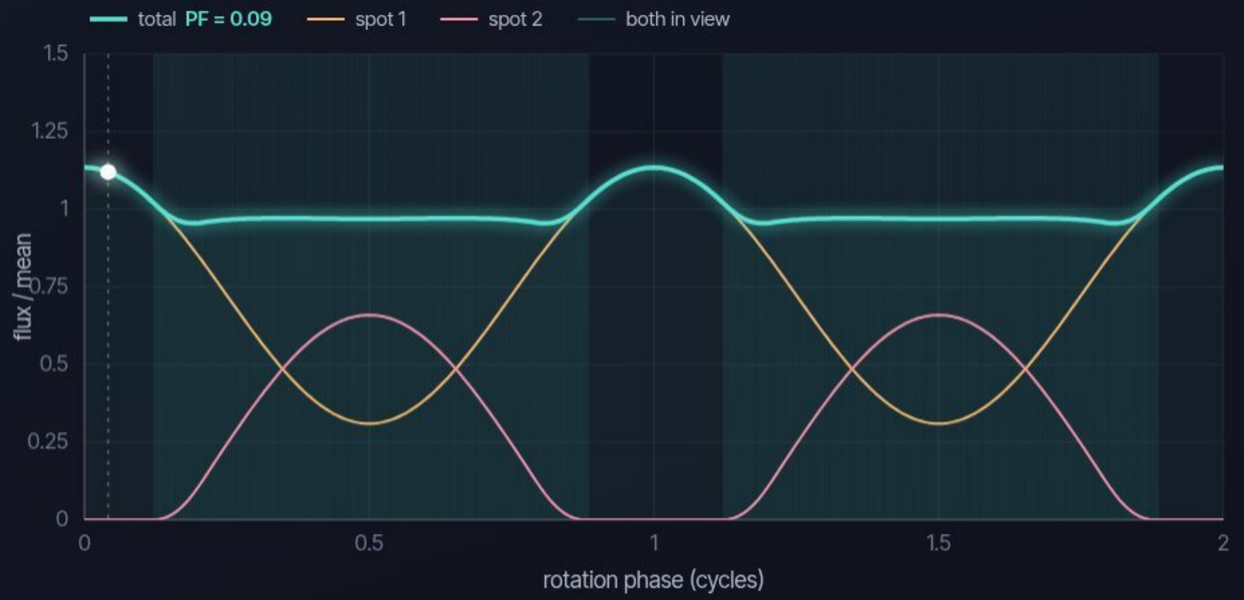
• TWO SPOTS: ONE AT EACH MAGNETIC POLE

antipodal | offset

• spot 1
• spot 2



1.4 M⊙ · 10 km · R = 2.42 R_s
exact integral · 1 turn per 4 s



magnetic axis ↔ rotation, *i* 45°

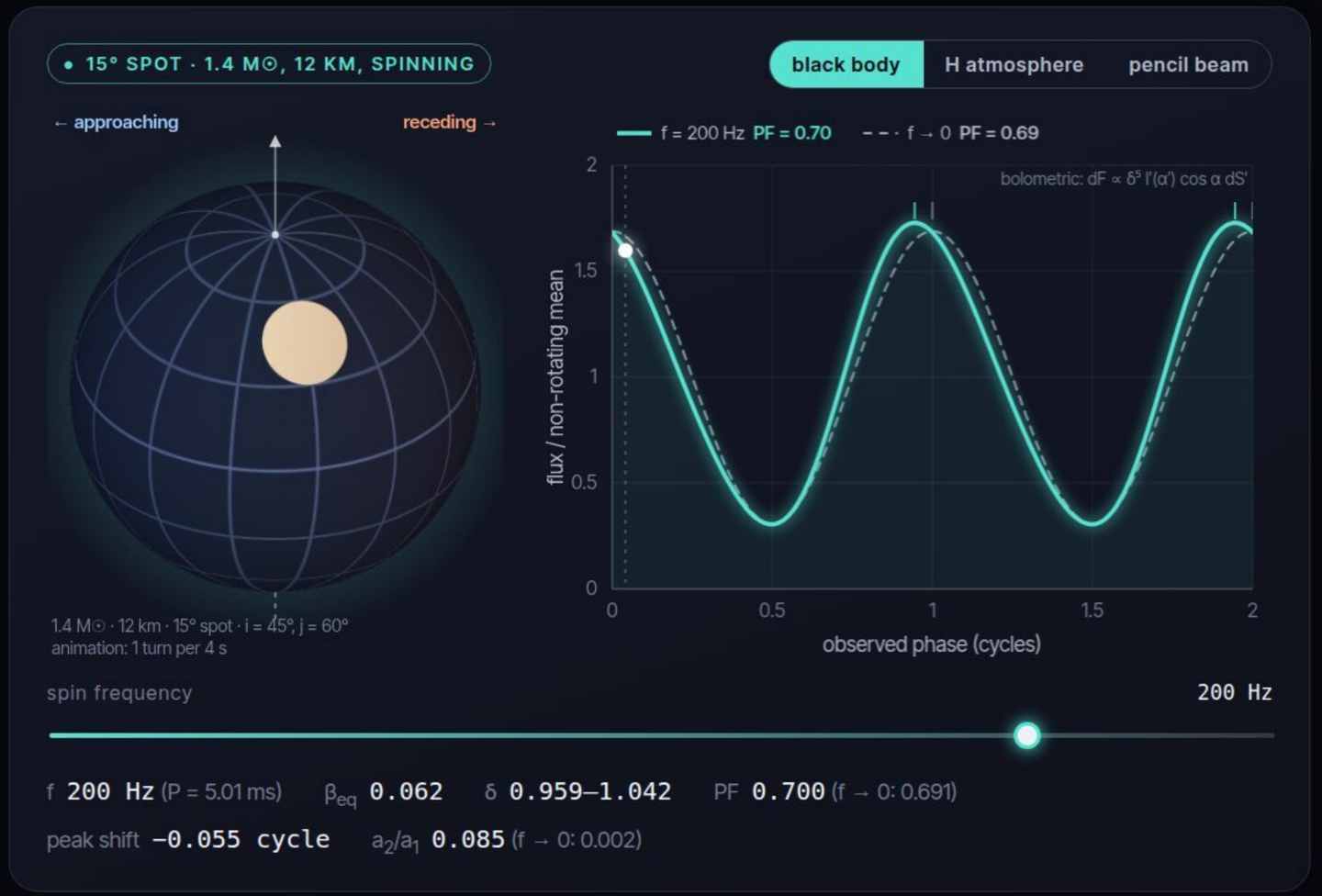
observer ↔ rotation, *j* 60°

offset of the second spot 0°

class **II** · primary always; antipodal sometimes PF **0.086** spot 1 in view **always** spot 2 in view **77% of the turn** both **77%** pulses separated by **0.50 cycle**

Ψ_{max} **131.9°**

Doppler, aberration, delays *and beaming*

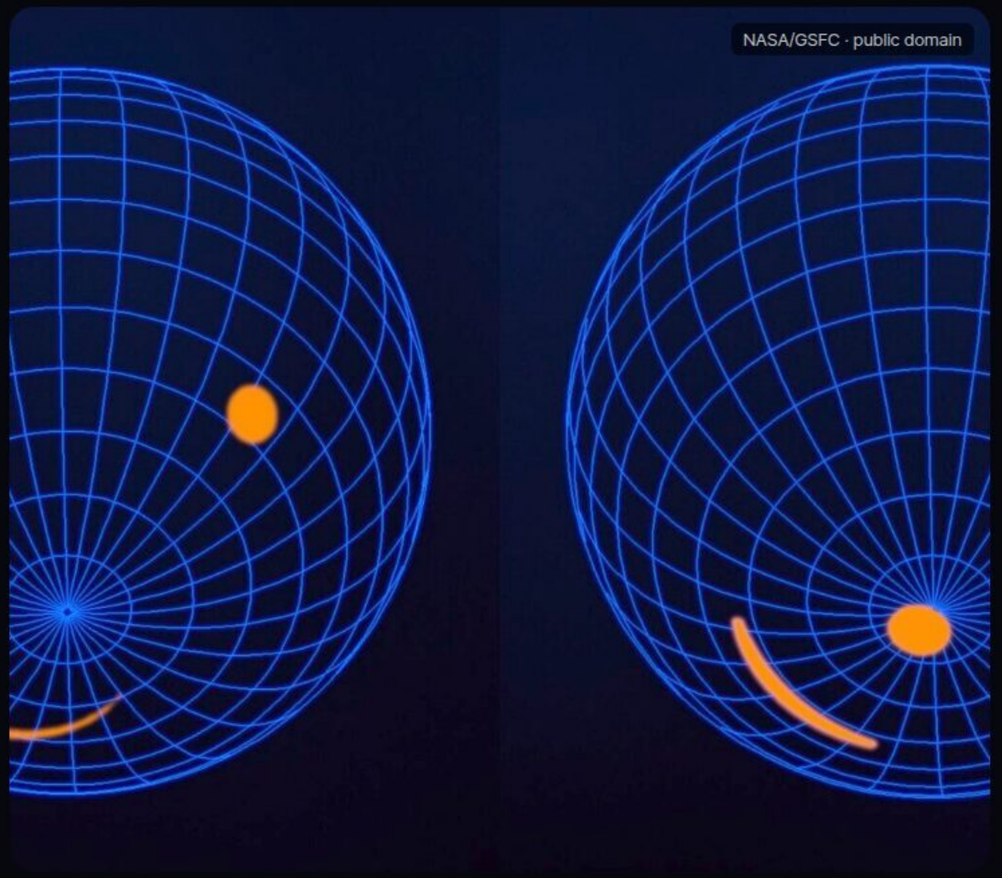


- **Doppler**: the surface moves at up to 0.1–0.2 c; the approaching side is brighter (bolometric flux ∝ δ^5).
- **Aberration**: the emission angle changes in the frame of the surface.
- **Delays**: tens of μs between points on the star — fractions of the period at hundreds of Hz.
- **Beaming**: an atmosphere does not emit equally in all directions; the profile depends on it.

Together they make the pulse **asymmetric** and create harmonics — and the asymmetry measures R separately from M.

NICER · PULSE-PROFILE MODELLING

Mass and radius *from the pulse shape*



PSR J0030+0451 · the solutions of the two teams: Amsterdam (Riley+ 2019, left) and Maryland (Miller+ 2019). In both, the spots are far from antipodal.

PULSAR	MASS (M⊙)	RADIUS (KM)
PSR J0030+0451 · Riley+ 2019	$1.34^{+0.15}_{-0.16}$	$12.7^{+1.1}_{-1.2}$
PSR J0030+0451 · Miller+ 2019	$1.44^{+0.15}_{-0.14}$	$13.0^{+1.2}_{-1.1}$
PSR J0740+6620 · Riley+ 2021	$2.07^{+0.07}_{-0.07}$	$12.4^{+1.3}_{-1.0}$
PSR J0437−4715 · Choudhury+ 2024	1.42 ± 0.04	$11.4^{+1.0}_{-0.6}$

NICER time-stamps each photon to ~100 ns. Folding millions of photons at the period gives the pulse profile; ray tracing, with M, R, the geometry and the spots left free, fits that profile by Bayesian inference.

J0030's spots came out non-antipodal and elongated: the field is not a centred dipole.

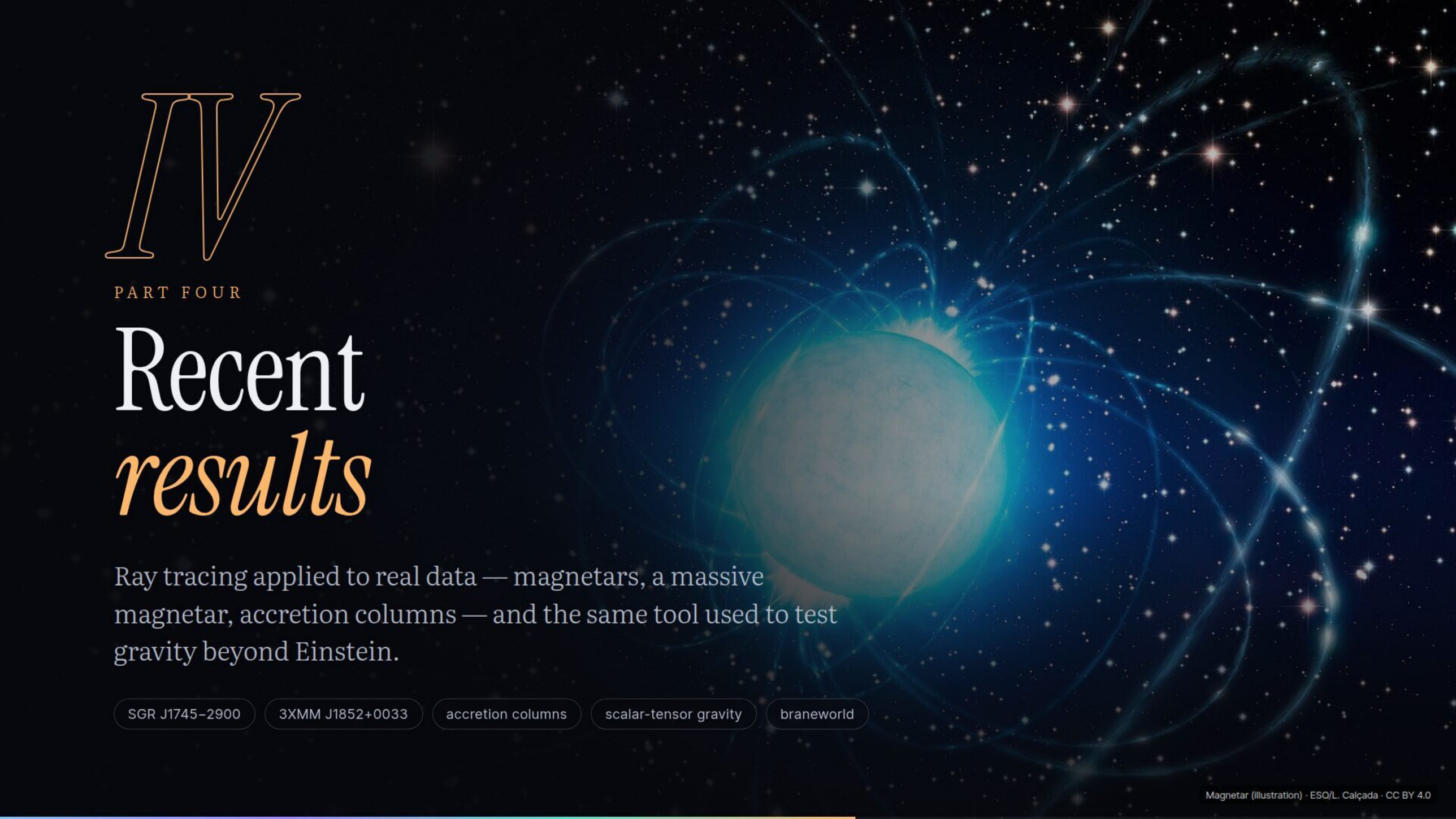
IV

PART FOUR

Recent *results*

Ray tracing applied to real data — magnetars, a massive magnetar, accretion columns — and the same tool used to test gravity beyond Einstein.

SGR J1745−2900 | 3XMM J1852+0033 | accretion columns | scalar-tensor gravity | braneworld



Magnetar (illustration) · ESO/L. Calçada · CC BY 4.0

2017 – 2026

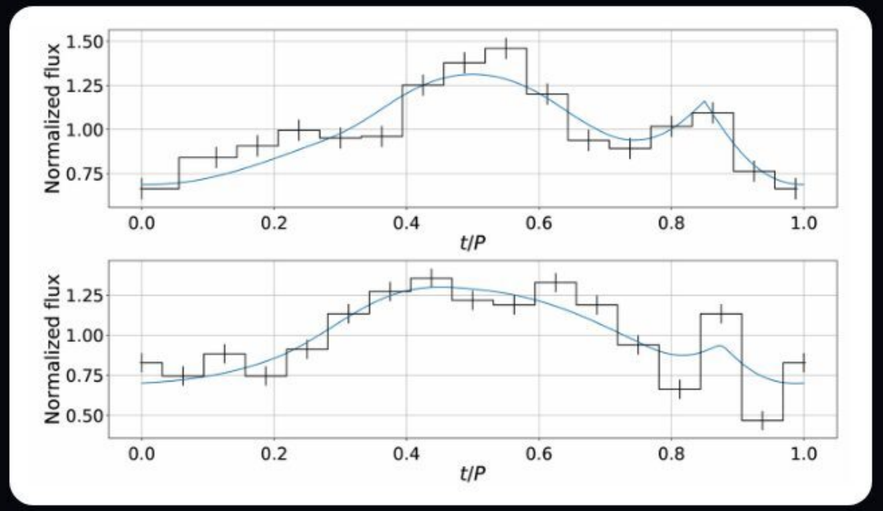
Light curves *as an instrument*

2017	2020	2023	2024	2024	2024	2025	2026	2026
A&A 599, A87: rotation-powered SGRs and AXPs, with realistic neutron stars	**ApJ 889, 165**: SGR J1745–2900 and a multipolar field, from the light curve	**Galaxies 11, 18**: pulse profiles of accretion columns	**JHEAp 42, 52**: 3XMM J1852+0033, a massive low-field magnetar	**EPJC 84, 1337**: light curves as a test of scalar-tensor gravity	**PRD 110, 103014**: stratified rotation and the moment of inertia	**PRD 112, 083010**: quark stars and the QCD equation of state	**arXiv:2607.09836**: compact stars in a high-tension braneworld	**JHEAp (submitted)**: the column of 1A 0535+262 through its NuSTAR spectrum

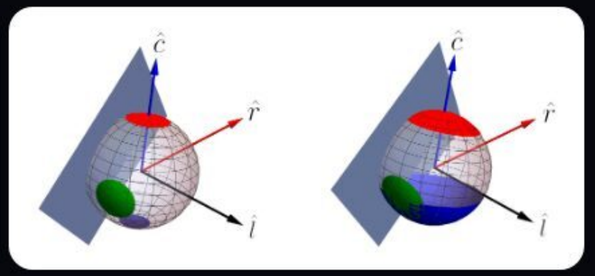
The common thread: reading in the light of a compact star its *mass*, its *radius*, its *field* — and the *gravity* that curves it.

DE LIMA, COELHO, PEREIRA, RODRIGUES & RUEDA · APJ 889, 165 (2020)

SGR J1745−2900: *more than two spots*



Chandra light curves (2013 and 2016) and the three-spot fits.



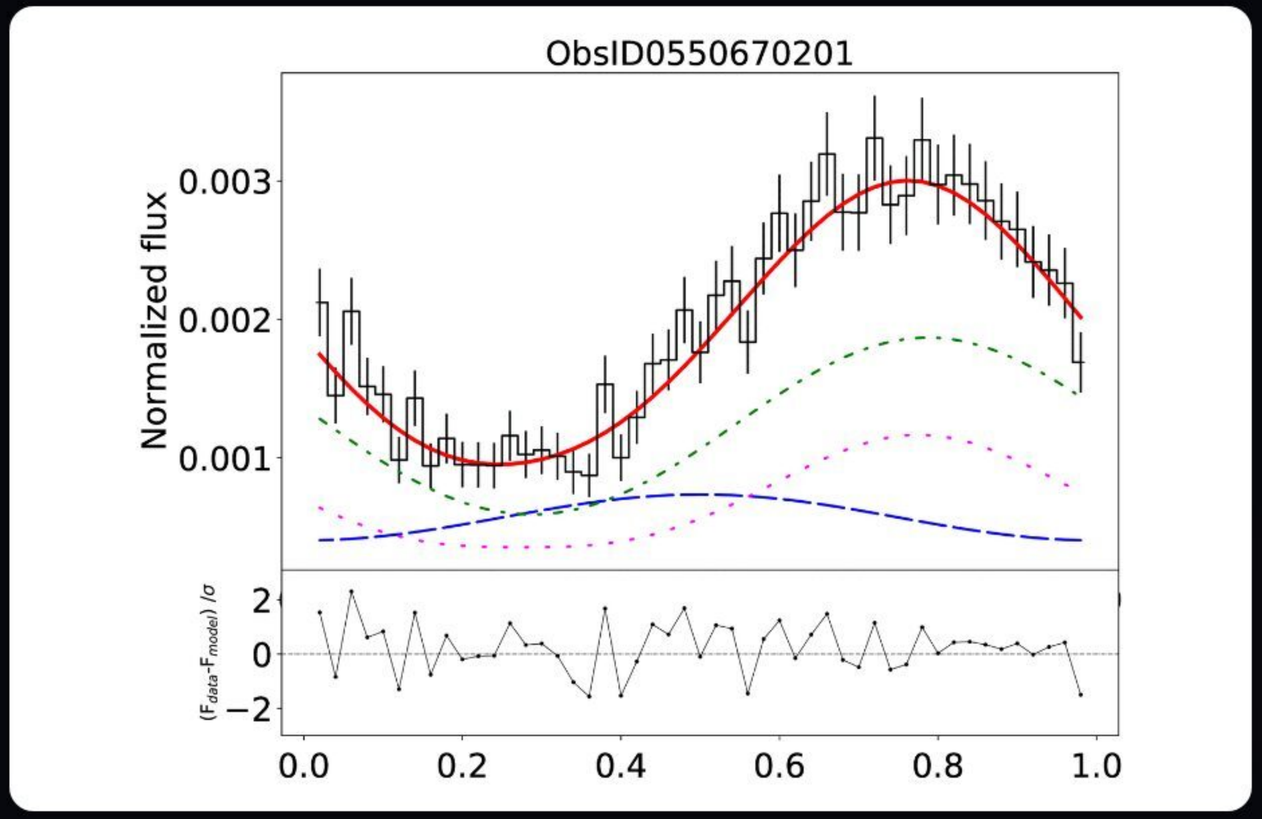
The three spots: two at the poles, one in the southern hemisphere.

- The magnetar 0.1 pc from Sgr A*; 3.5 years of **Chandra** data.
- Model: M, R, up to **three spots** of any size and position, Schwarzschild light bending; fitted with a genetic algorithm.
- Two or three spots describe the data; with three, they are **large** (16–67°).
- A field with non-trivial poloidal and toroidal structure — the same message NICER gave for J0030.

1.4 ± 0.1	10.9 ± 1.5
$M_\odot$	km

DE LIMA ET AL. · JHEAP 42, 52 (2024) · 1/2

3XMM J1852+0033: *ray tracing and inference*



One of the five pulse profiles (XMM-Newton, 2008) and the best fit: dashed, the contribution of each spot.

- A **transient magnetar** near the remnant Kes 79, P = 11.56 s; until then there were only upper limits on the field.
- Five **XMM-Newton** epochs over three weeks in 2008.
- **Ray tracing** in Schwarzschild with circular spots of any size (Turolla & Nobili 2013) and **magnetised atmospheres** (NSMAX: H, C, O), with anisotropic emission.
- **Bayesian inference** (MCMC): mass, radius, field and spot positions shared by all epochs; size and temperature free to vary.
- Tested by **injection and recovery** of simulated data.

BEST MODEL

Three small spots, two in the southern hemisphere, and a **carbon** atmosphere: $\chi^2/\mathrm{dof} = 1.22$, well ahead of two spots or of hydrogen.

A *massive*, low-field magnetar

$2.09^{+0.16}_{-0.09}\ M_\odot$

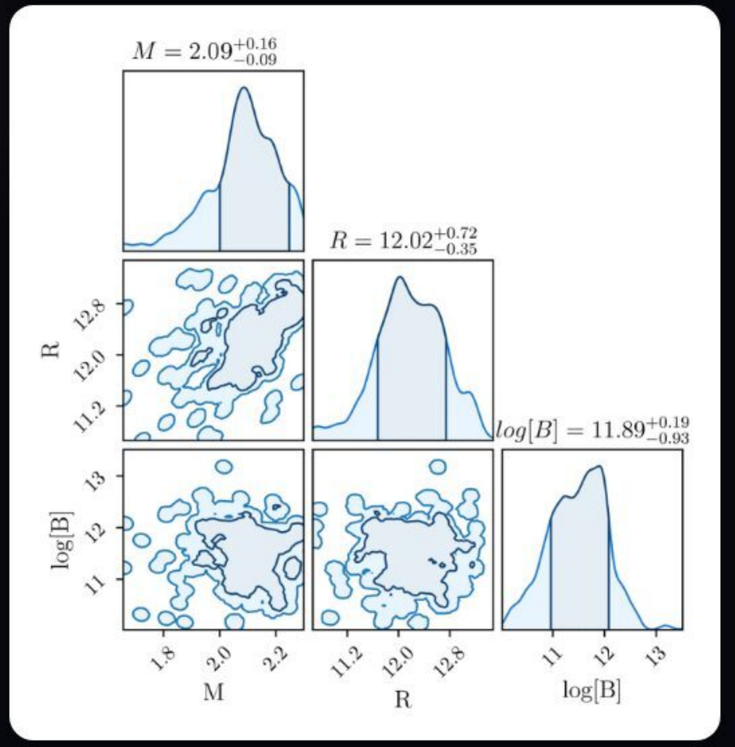
mass (1σ): among the highest ever estimated

12.0 ± 1.4 km

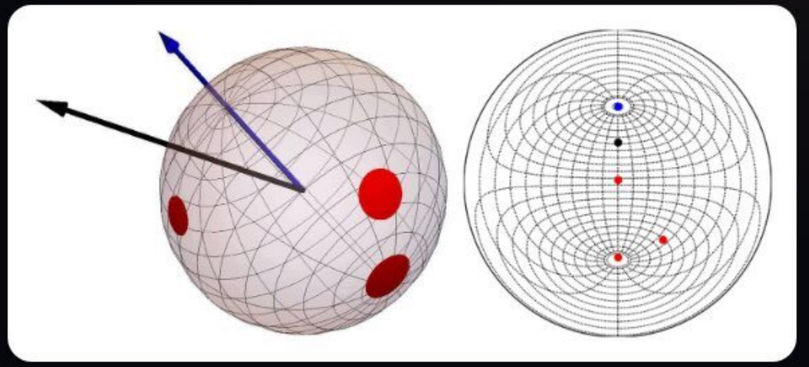
radius (2σ)

$\sim 8 \times 10^{11}$ G

surface field: log B = $11.89^{+0.19}_{-0.93}$, below the critical value



Posteriors of *M*, *R* and log *B*.



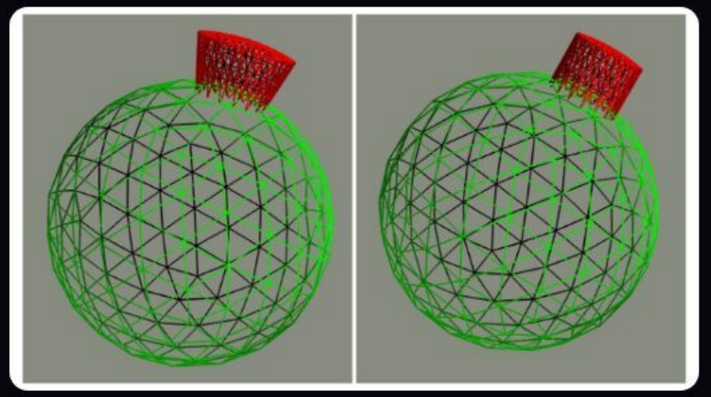
The best-fit geometry.

Interpretation: accretion of supernova material **buried** the field, which is now re-emerging; the carbon atmosphere would come from diffusive nuclear burning of H/He.

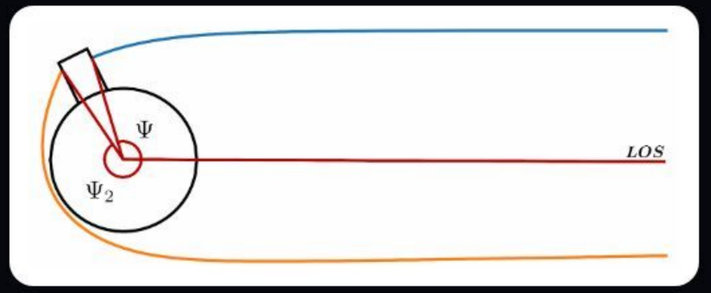
Compactness $GM/Rc^2 \approx 0.26$: favours equations of state of intermediate stiffness.

SILVA, DE LIMA, COELHO, STECCHINI, DE LIZ & DE ARAUJO · GALAXIES 11, 18 (2023)

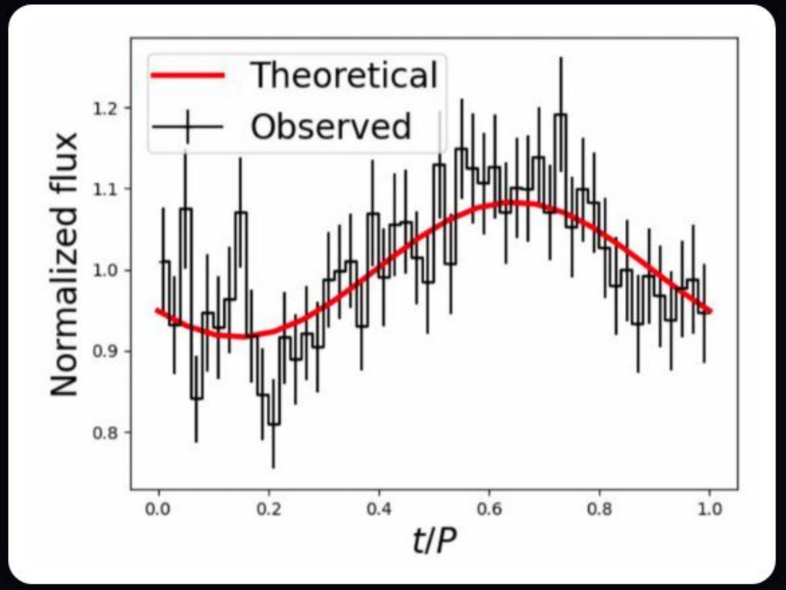
When the light comes *from a column*



The star and the columns (truncated cone and cylinder) as a 3D mesh.



Photons emitted above the surface may pass through a **periastron** before escaping.



1A 0535+262 (NuSTAR, 2018): observed profile and the two-column model.

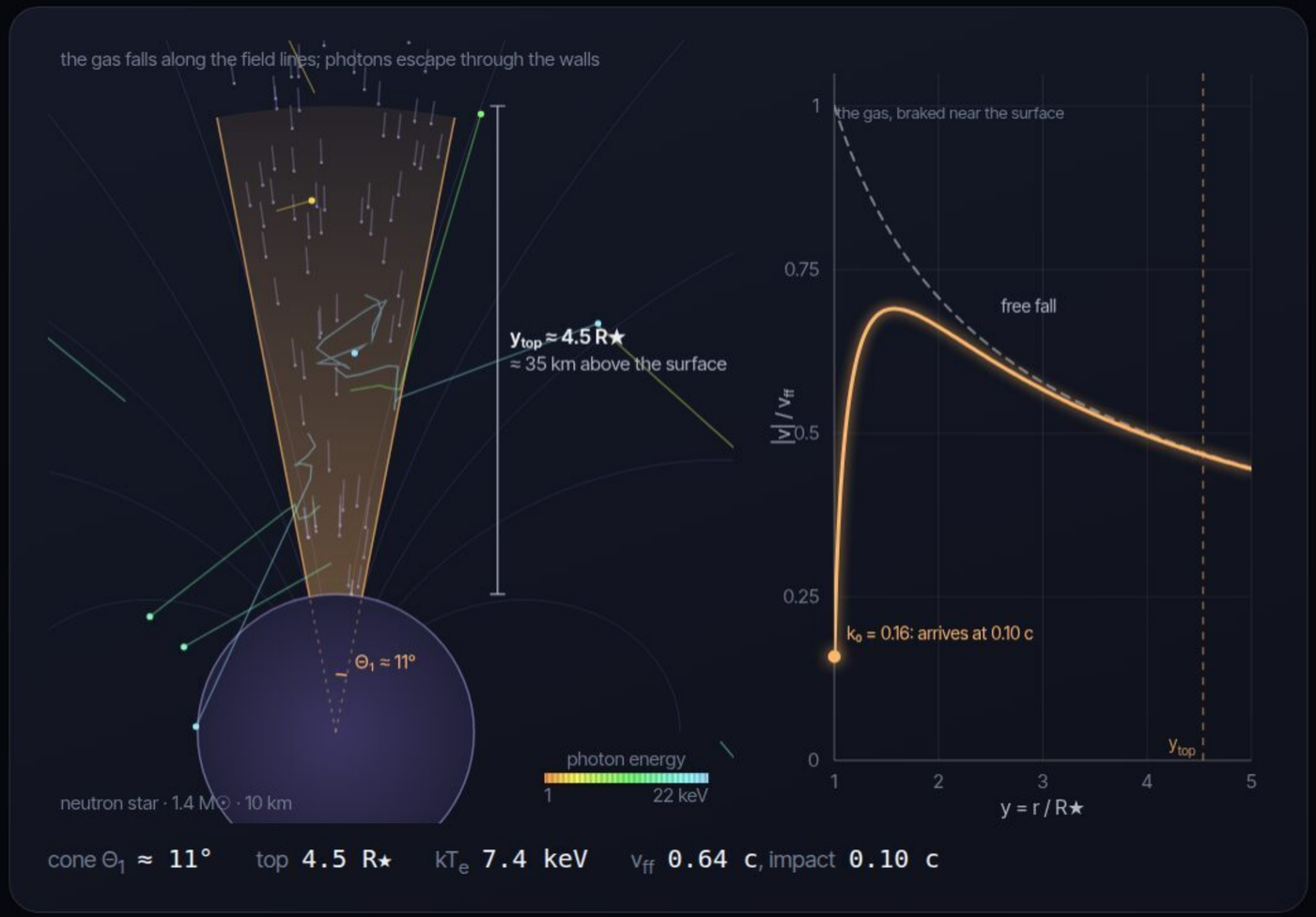
- In X-ray binaries, matter falls along the field lines and forms **columns** above the poles: the emission comes out sideways (fan beam).
- **Exact** ray tracing in Schwarzschild, tabulated, including for points above the surface; Doppler included.
- Genetic algorithm for the priors, then MCMC.

$1.53^{+0.52}_{-0.40}$ $M_\odot$

$12.1^{+1.1}_{-0.9}$ km

SILVA, DE LIMA, COELHO & DE ARAÚJO · SUBMITTED TO JHEAP (2026) · THE MODEL

Inside the column, *through the spectrum*

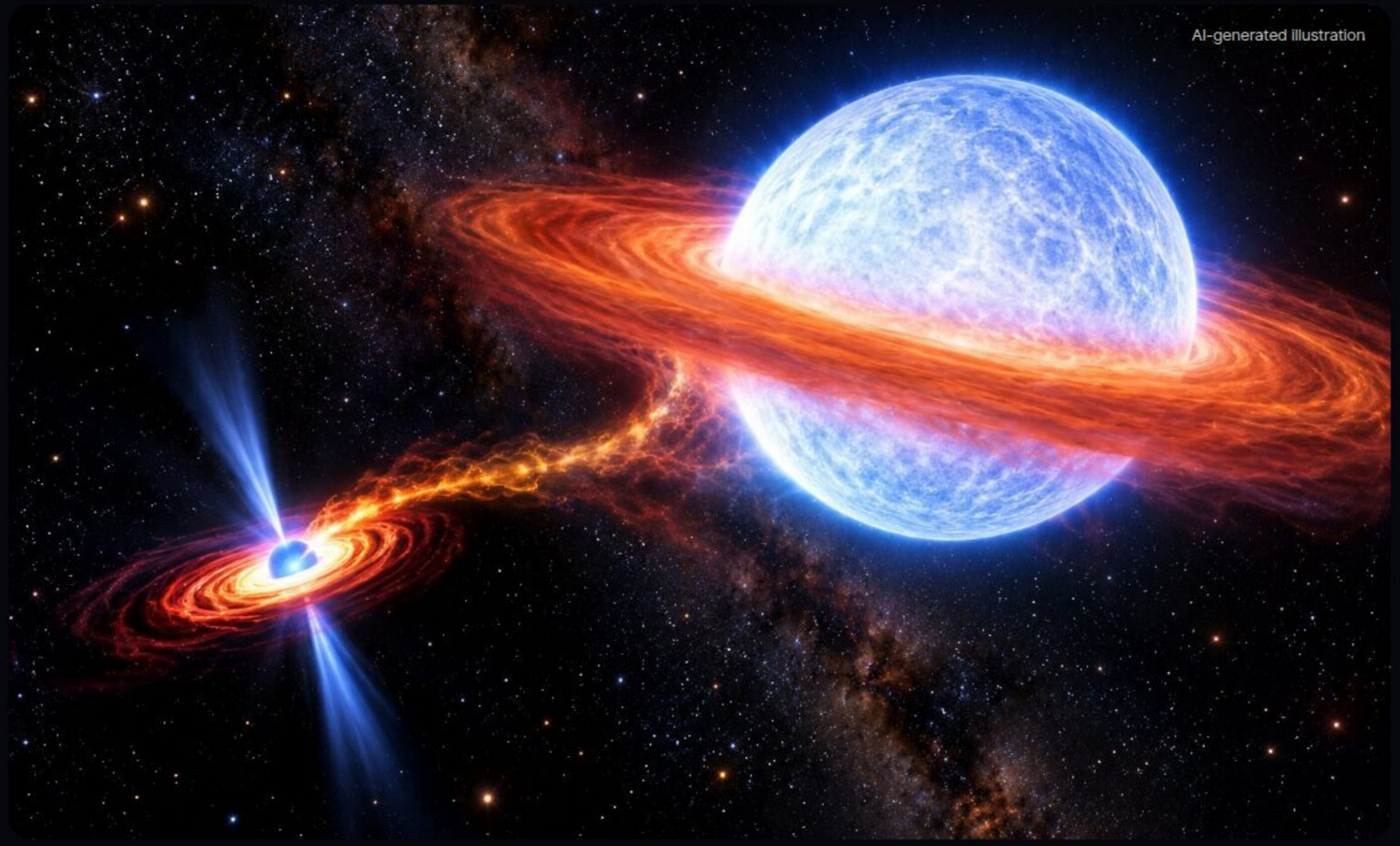


- The same star as on the previous slide, now through its **spectrum**: NuSTAR, 3–44 keV, $L \approx 3.7\times10^{36}$ erg/s — 16 times below the critical luminosity.
- **Becker & Wolff (2022)** model: a conical column; photons gain energy from the hot electrons and from the infalling gas (thermal and *bulk* Comptonization) and escape through the walls.
- 12 parameters, 4 independent MCMC chains of 256 walkers. The posterior has **two modes**; the dominant one wins by $\Delta\ln\mathcal{P} \approx 55$.

$$v(y) = -v_{ff}\left[\frac{k_\infty^2(y^3-1)+k_0^2}{y^4}\right]^{1/2}$$

y = r/R★ · FREE FALL HIGH UP, BRAKED NEAR THE SURFACE

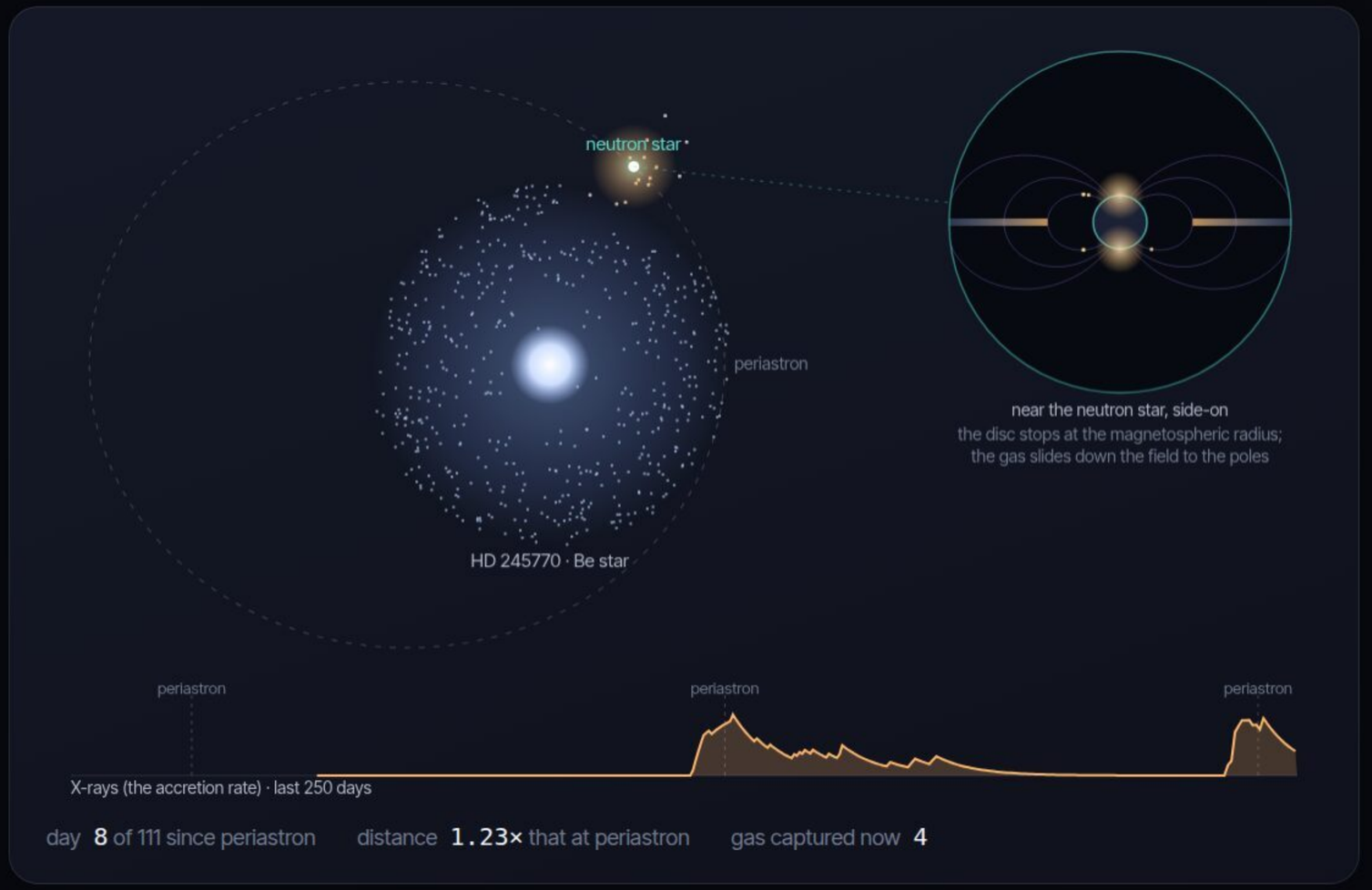
A Be star: *a disc at the equator*



A Be/X binary: the Be star's disc, the gas torn from it and the accretion disc around the neutron star.

- **Be** stars: hot, of type B and late O, spinning close to break-up and losing gas from the equator, which forms a **disc**.
- The "e" in O9.7–B0 III**e** stands for the hydrogen emission lines, such as Hα, which come from the disc; a double-peaked profile shows it rotates.
- In 1A 0535+262 the companion is the **neutron star**, on a 111-day orbit that crosses the edge of the disc — the next slide.

Where *the column's gas* comes from



- **1A 0535+262**: a neutron star pulsing every 103 s, with $B \approx 5\times10^{12}$ G, on an eccentric orbit — $e \approx 0.45$, 111 days — around **HD 245770**, a Be star (O9.7–B0 IIIe), at 1.8 kpc.
- The Be star spins fast and sheds a **disc of gas** from its equator.
- At periastron the neutron star crosses the edge of the disc and **steals gas**: an X-ray outburst every orbit.
- Close to it, the field cuts the disc at the magnetospheric radius and leads the gas to the poles: **the columns**.

In 2020 a giant outburst reached 1.2×10^{38} erg/s; in quiescence, $\sim7\times10^{34}$ erg/s. The orbit has the system's eccentricity and period; the stars, the disc and the close-up are schematic.

One equation for *the photons in the column*

$$v\frac{\partial f}{\partial R} = \frac{\varepsilon}{3R^2}\frac{\partial (R^2 v)}{\partial R}\frac{\partial f}{\partial \varepsilon} + \frac{1}{R^2}\frac{\partial}{\partial R}\left(\frac{R^2 c}{3 n_e \sigma_{\parallel}}\frac{\partial f}{\partial R}\right) + \frac{n_e \sigma \bar{c}}{m_e c^2}\frac{1}{\varepsilon^2}\frac{\partial}{\partial \varepsilon}\left[\varepsilon^4\left(f + kT_e\frac{\partial f}{\partial \varepsilon}\right)\right] - \frac{f}{t_{esc}} + Q(R,\varepsilon)$$

STEADY-STATE TRANSPORT EQUATION FOR THE PHOTON DISTRIBUTION, $f(R, \varepsilon)$ · BECKER & WOLFF (2022), CONICAL GEOMETRY

ADVECTION
the infalling gas carries the photons along, with the $v(y)$ of the previous slide

***BULK* COMPTONIZATION**
the flow converges: scattering off the infalling gas, photons gain energy

DIFFUSION
photons move along the column, with the strong-field cross section $\sigma_{\parallel}$

THERMAL COMPTONIZATION
the Kompaneets term: electrons at T_e drive the spectrum towards ~kT_e

ESCAPE
photons leave through the walls in a time t_{esc}: the fan beam

SOURCES
seed photons: bremsstrahlung, cyclotron and blackbody from the base

HOW IT IS SOLVED

$$f_G = \Sigma_n C_n g_n(\tau)\left(\frac{\varepsilon}{kT_e}\right)^{\kappa-4} e^{-\varepsilon/2kT_e} M_{\kappa,\mu}\left(\frac{\varepsilon_{min}}{kT_e}\right) W_{\kappa,\mu}\left(\frac{\varepsilon_{max}}{kT_e}\right)$$

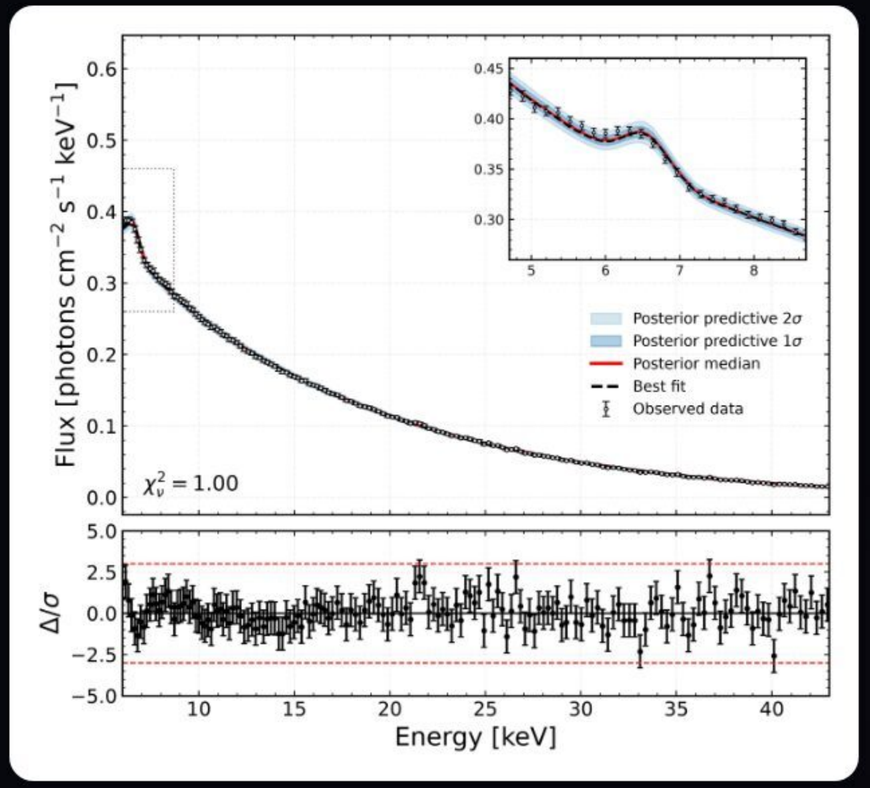
Separation of variables: eigenfunctions $g_n(\tau)$ in optical depth and Whittaker functions in energy. The spectrum is this Green's function convolved with the sources, adding the wall and the top of the column. Magnetic cross sections with vacuum polarization; cyclotron and iron lines, empirical. The implementation was checked equation by equation.

WHAT THE MCMC SAMPLES: 12 PARAMETERS

α velocity · ξ diffusion · ψ bulk/thermal · θ_0 opening · k_0 impact · y_{top} height · T_e electrons · $\dot{M}$ accretion · B field · d_{Fe} iron · f_{sys} systematics · D distance

Fixed: $M = 1.4\ M_\odot$, $R_\star = 10$ km, N_H and the cyclotron line, outside the band. B has a prior from the line (46.3 keV). The likelihood is Gaussian, with the systematic term f_{sys}, and charges the energy budget $L_{acc} = GM\dot{M}/R_\star$ within a factor of 2.

A hot, tall column — *and a missing piece*



The NuSTAR spectrum and the posterior (median and 1σ and 2σ bands), with the residuals. Inset: the iron line.

$8.56_{\times 10^7\,\mathrm{K}}$

electron temperature, to 1% · $kT \approx 7.4$ keV

$4.5\,R_\star$

top of the column, ~35 km above the surface

0.070

ψ, bulk/thermal: **thermal** Comptonization dominates

$\log \theta_0 - 1.36 \log \dot{M} = -22.32 \pm 0.10$

the spectrum fixes the combination: more $\dot{M}$, a wider column

A MISSING PIECE

The field comes out 2.3σ above that of the cyclotron line — which would then sit at 55 keV, not the measured 46 — and the residuals move together (runs test: z = −3.7). Candidate: recombination between excited Landau levels, seen in this source and absent from the model.

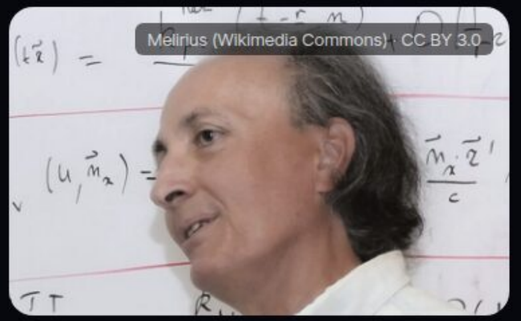
Dominant posterior mode. $\chi^2_\nu = 1.00$ with a free systematic uncertainty is not a goodness-of-fit test: the residuals are the diagnostic.

BRANS & DICKE 1961 · DAMOUR & ESPOSITO-FARÈSE 1993

What if gravity *is not Einstein's?*



Carl Brans
1935 – 2022



Thibault Damour
b. 1951

WHAT "COUPLING TO MATTER" MEANS

$$\tilde{g}_{\mu\nu} = A^2(\varphi)\, g_{\mu\nu}$$

THE METRIC MATTER FEELS

Matter measures distances and times with $\tilde{g}$: its rulers and clocks change with ϕ. Light does not notice — a conformal change leaves null geodesics alone — but the radius matter measures is $R = A_s R_E$.

$$\alpha(\varphi) = \frac{d \ln A}{d\varphi}$$

THE STRENGTH OF THE COUPLING

Matter sources the field, $\Box\phi = -4\pi G\alpha T$, and feels an extra force, $\propto \alpha\nabla\phi$: between two bodies, $G_{\text{eff}} = G(1 + \alpha^2)$.

In **scalar-tensor** theories, besides the metric there is a scalar field ϕ that couples to matter. In the Solar System the coupling is tiny ($\alpha^2 < 10^{-5}$, from the Cassini probe); in a neutron star **spontaneous scalarisation** can occur: with $A = e^{\beta\phi^2/2}$ and $\beta \lesssim -4.35$, $\phi = 0$ becomes unstable and the field grows on its own, like spontaneous magnetisation.

Outside the star, the metric is no longer Schwarzschild: it is the **Just metric**, with a scalar charge Q:

$$ds^2 = -\left(1 - \frac{a}{r}\right)^{b/a} dt^2 + \left(1 - \frac{a}{r}\right)^{-b/a} dr^2 + \left(1 - \frac{a}{r}\right)^{1-b/a} r^2 d\Omega^2$$

$b = 2GM/c^2 \cdot a/b = \sqrt{(1 + Q^2)}$ · EINSTEIN FRAME

Two stars with the **same mass and the same radius** — "doppelgängers" — bend light in different ways. The light curve can tell the theories apart.

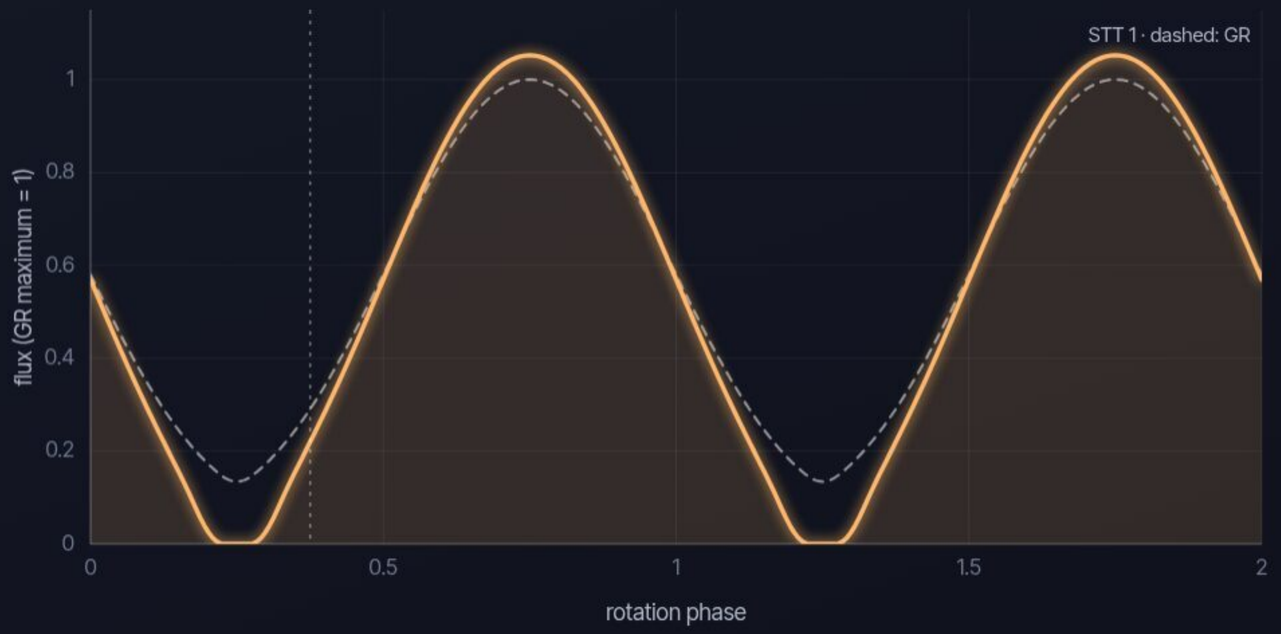
The same star, *different gravity*

• M = 2.1 M⊙ · ONE 10° SPOT · ι = θ = 90° · STATIC STAR · EXACT INTEGRAL

GR | STT 1 · A_s = 0.95 | STT 2 · A_s = 1.05

the star seen from afar · dashed: its size in GR



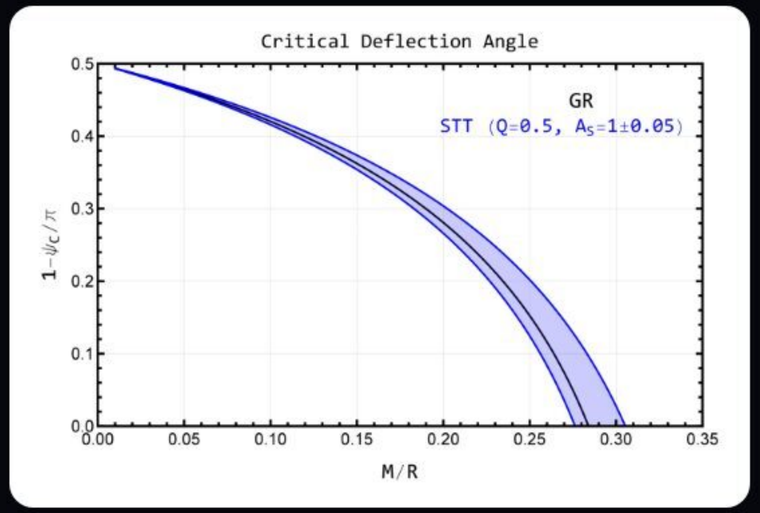


compactness, GM/Rc^2 0.284

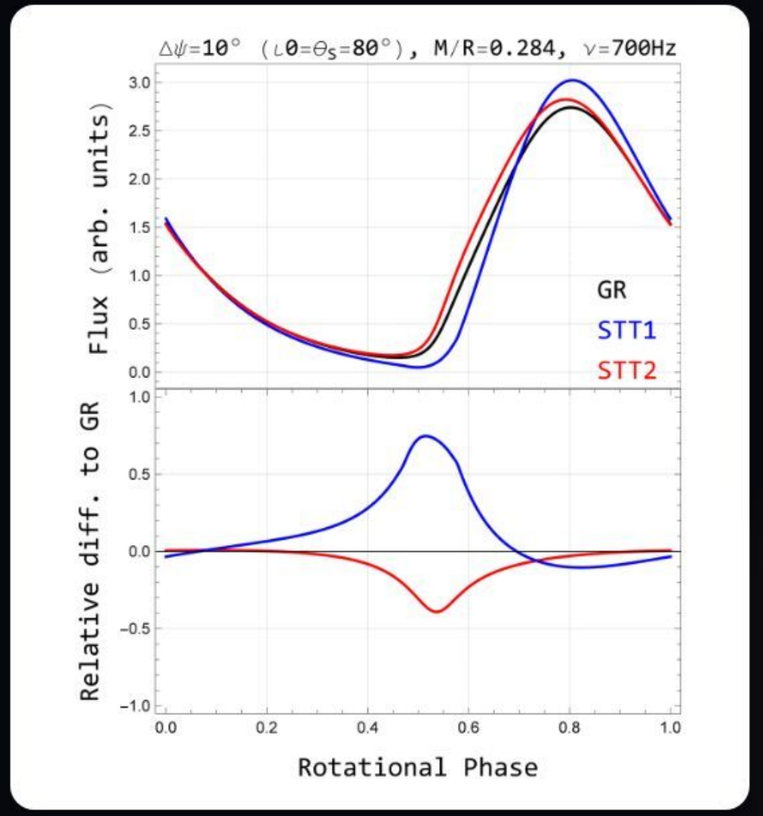
scalar charge, Q 0.50

STT 1: ψ_c 0.903π GR: ψ_c 1.000π invisible zone 17.4° R 10.92 km apparent radius 16.88 km PF 1.00

Up to *80%* difference in flux



The critical angle versus *M*/*R*: the GR line and the scalar-tensor band.



Spinning at 700 Hz, with Doppler and delays: flux and difference relative to GR.

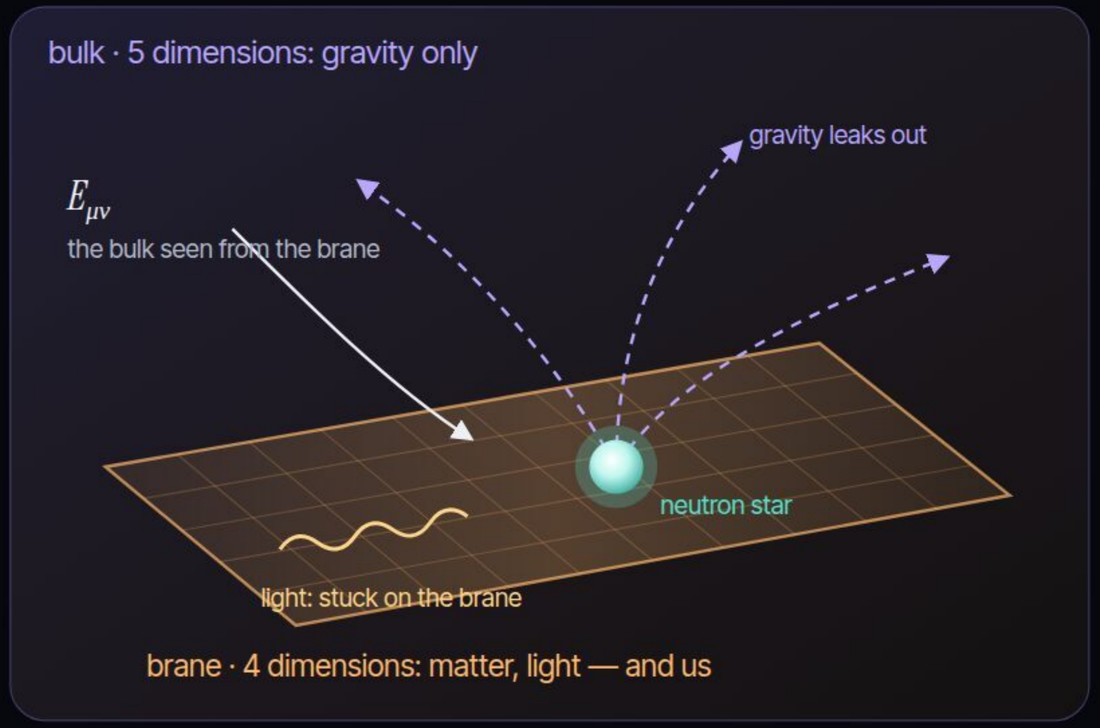
- The compactness at which $\psi_c = \pi$ ranges from **0.275 to 0.305** in scalar-tensor theory, against 0.284 in GR.
- The flux from a spot differs from GR by up to **~80%**.
- The radius changes by up to **~10%** for the same stellar parameters: today, this limits $Q \lesssim 0.5$.
- With NICER, J0740+6620 has $C = 0.21$–0.28: not yet enough to separate the theories.

OUTLOOK

Radii with smaller uncertainties — eXTP, NewAthena, and gravitational waves from Einstein Telescope and LISA — may constrain scalar-tensor theories through the **pulse shape**.

RANDALL & SUNDRUM 1999 · SHIROMIZU, MAEDA & SASAKI 2000

The Universe on a *membrane*



In a **braneworld**, our Universe is a four-dimensional hypersurface — the **brane** — inside a space with one extra dimension, the **bulk**. Matter and light are stuck on the brane; only gravity propagates in the bulk.

The idea was put forward to attack the hierarchy problem (why gravity is so weak) and the cosmological-constant problem and accelerated expansion.

$$G_{\mu\nu} = 8\pi T_{\mu\nu} + \frac{48\pi}{\lambda} S_{\mu\nu} - E_{\mu\nu}$$

SHIROMIZU, MAEDA & SASAKI 2000 · $\kappa_5^4 = 48\pi/\lambda$ ($G = c = 1$)

- $S_{\mu\nu}$: **local** corrections, quadratic in the matter ($\propto T^2$). In a fluid they add $\rho^2/2\lambda$ to the density: they matter when ρ approaches the **brane tension** λ.
- $E_{\mu\nu}$: the bulk **Weyl** tensor projected onto the brane — **nonlocal**: it cannot be computed from brane quantities alone.
- For $\lambda \to \infty$ and $E_{\mu\nu} \to 0$, General Relativity is recovered.

In the paper: an effective 4D closure, inspired by the Sahni–Shtanov scenario (2003) — not a complete 5D bulk solution.

Same nuclear physics, *different gravitation*

The equation of state of the matter (SLy) **does not change**. What changes is how much it **gravitates**: the star now feels an effective density and pressure.

$$\rho_{\text{eff}} = \rho + \frac{\rho^2}{2\lambda} + \rho_{\mathcal{W}}$$
$$p_{\text{eff}} = p + \frac{p\rho}{\lambda} + \frac{\rho^2}{2\lambda} + p_{\mathcal{W}}$$

LOCAL TERM (λ) · WEYL SECTOR ($\mathcal{W}$)

$$\frac{dm}{dr} = 4\pi r^2 \rho_{\text{eff}}$$
$$\frac{dp}{dr} = -(\rho + p)\,\frac{m + 4\pi r^3 p_{\text{eff}}}{r(r - 2m)}$$

MATTER IS CONSERVED: THE $(\rho + p)$ FACTOR IS THE USUAL ONE

The local term **strengthens attraction** and shrinks the star — but only when ρ approaches λ. At the centre of a neutron star $\rho \approx 2\times10^{-3}$ km^{-2}; with $\lambda \sim 10^{4}$ km^{-2}, $\rho/\lambda \sim 10^{-7}$.



WHAT COMES FROM THE BULK

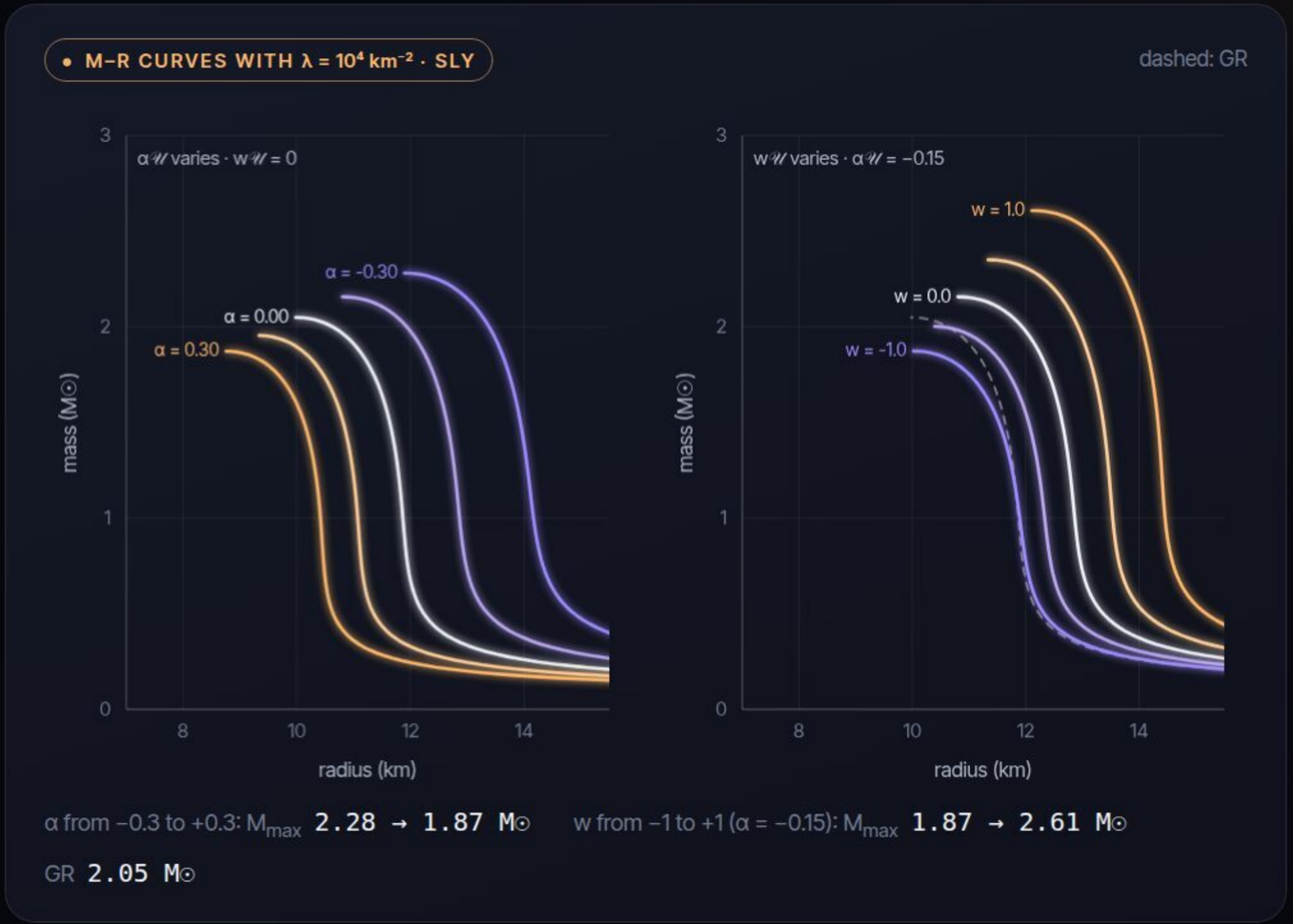
The Weyl sector: *screening* or extra attraction

$E_{\mu\nu}$ is the imprint of the bulk's gravitational field on the brane. There it acts as an **effective fluid** — in cosmology, the "dark radiation". But the brane does not determine this fluid: a **closure** is needed.

$$\rho_{\mathscr{W}} = \alpha_{\mathscr{W}}\,\rho \qquad p_{\mathscr{W}} = w_{\mathscr{W}}\,\rho_{\mathscr{W}}$$

Isotropic closure; the anisotropic Weyl stress ($\Delta_{\mathscr{W}}$) is left for future work.

IF…	EFFECT ON THE STAR
$\alpha_{\mathscr{W}} < 0$	$\rho_{\text{eff}} = \rho(1+\alpha_{\mathscr{W}}) < \rho$: **screening** — less mass gravitates, larger and heavier stars
$\alpha_{\mathscr{W}} > 0$	more attraction: smaller and lighter stars
$w_{\mathscr{W}}$	only appears as $w_{\mathscr{W}}\alpha_{\mathscr{W}}\rho$ in the effective pressure: it matters little when $\alpha_{\mathscr{W}}$ is small, and it can **compensate** $\alpha_{\mathscr{W}}$

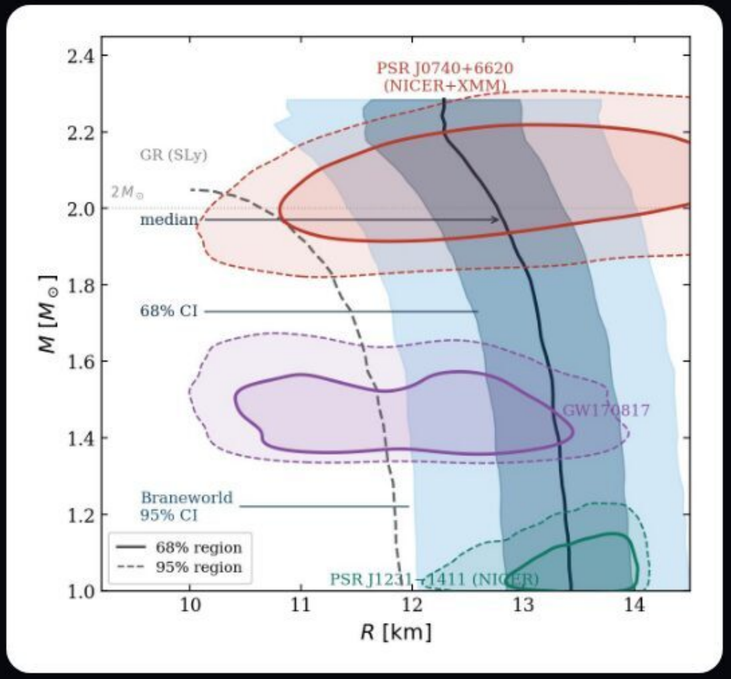


High tension, *mildly negative* Weyl coupling

DATA AND INFERENCE

GW170817 (radii from the tidal deformability) + NICER: PSR J0740+6620 and PSR J1231–1411 — both of them results of pulse-profile **ray tracing**. Ensemble MCMC (4 × 32 walkers × 3,000 steps, 288,000 samples), priors centred at large λ and at the GR values.

	MEDIAN	68%	GR
$\log_{10}(\lambda/\mathrm{km}^{-2})$	3.98	2.54 – 5.50	∞
$\alpha_{\mathcal{W}}$	−0.15	−0.23 – 0.15	0
$w_{\mathcal{W}}$	0.24	−0.78 – 0.61	0
$M_{\max}$ (M⊙)	2.30	2.22 – 2.44	2.05
$R_{1.4}$ (km)	13.31	12.74 – 13.85	11.76



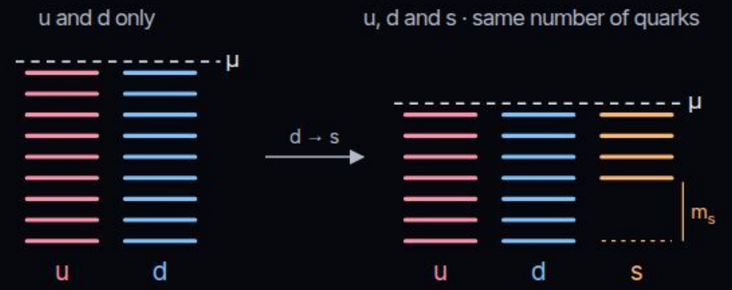
The posterior M–R band (68% and 95%), GR+SLy (dashed) and the constraints used.

- **$\lambda \sim 10^4$ km^{-2}**: the local term vanishes ($\rho/\lambda \sim 10^{-7}$). The posterior nearly repeats the prior: the data are *compatible* with high tension, they do not measure λ.
- **$\alpha_{\mathcal{W}} < 0$ in 83% of the samples**: a mild screening. It is the Weyl sector, not the local term, that pushes the curve to the right.
- **A secondary branch (17%)**: $\alpha_{\mathcal{W}} > 0$ and $w_{\mathcal{W}} < 0$ compensate — smaller $R_{1.4}$, larger $M_{\max}$, compactness near the imposed bound.
- **$M_{\max} \approx 2.3$ M⊙**: consistent with PSR J0952–0607 (2.35 ± 0.11 M⊙). GW190814 (2.50–2.67 M⊙) only fits in the 95% tail.
- **The message**: heavier stars are not a generic prediction of braneworlds — they depend on the **sign of the Weyl sector**.

ITOH 1970 · BODMER 1971 · WITTEN 1984 · THE STRANGE MATTER HYPOTHESIS

What if iron is *not* the bottom of the well?

At extreme densities neutrons may dissolve into quarks. The Bodmer–Witten hypothesis goes further: matter made of **u, d and s** quarks would be the **ground state** of matter — with an energy per baryon below that of ^{56}Fe, 930 MeV.



Pauli: each flavor has its own Fermi sea. A third flavor opens new levels and the top (μ) drops — even after paying for the s mass.

- Nuclei don't decay because that would take ~A **simultaneous** weak d → s conversions.
- And u–d matter alone must be **unstable** — otherwise iron itself would have turned into quarks.
- If it holds, "neutron stars" may be **quark stars**, bound by the strong force.



Dense QCD in *three numbers*

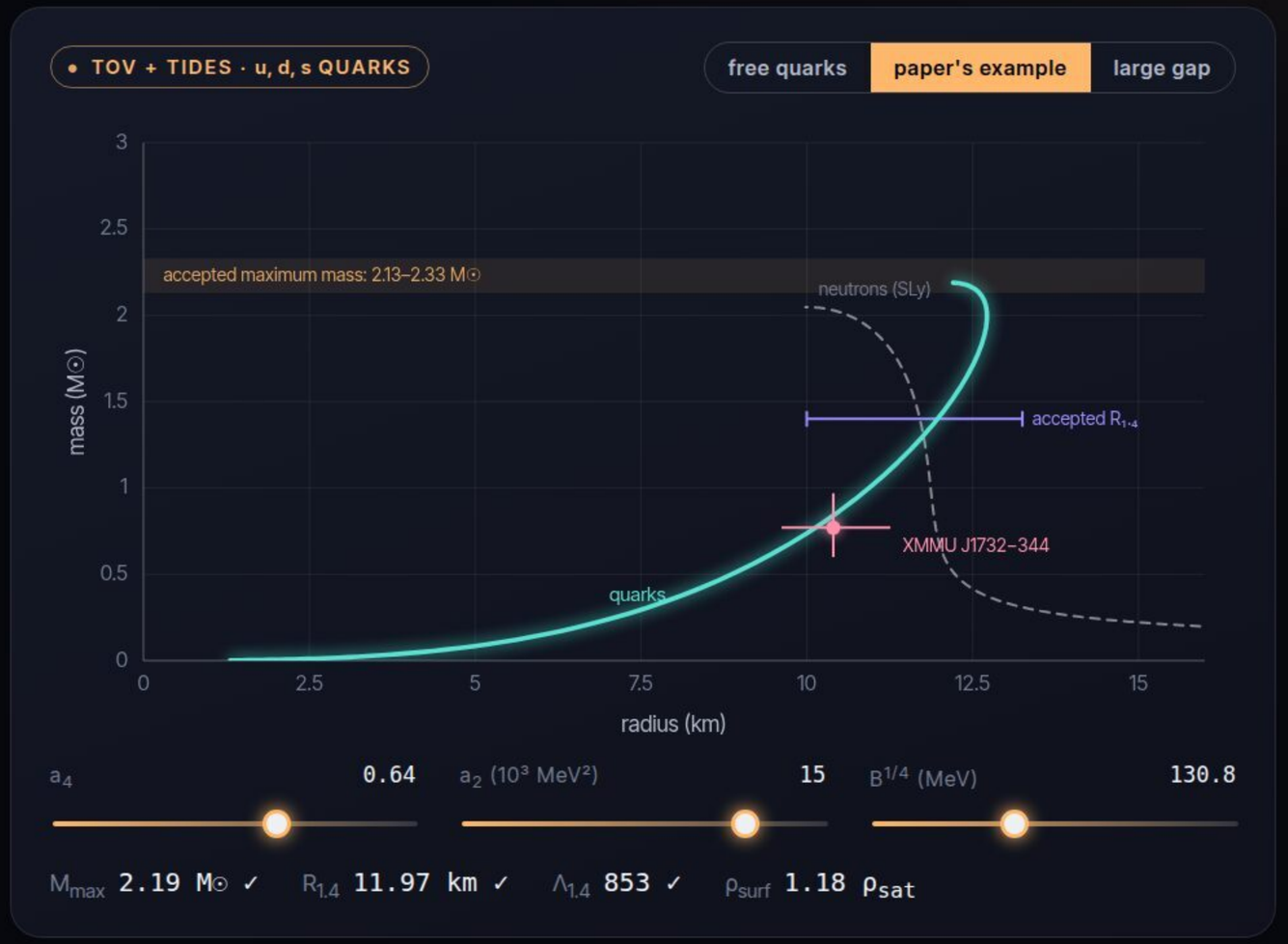
$$\omega = -\frac{3a_4}{4\pi^2}\mu^4 + \frac{3a_2}{4\pi^2}\mu^2 + B$$

THERMODYNAMIC POTENTIAL · $p = -\omega$ · μ: QUARK CHEMICAL POTENTIAL

$a_4 = 1 - c$	the **strong interaction**. $a_4 = 1$ means free quarks; perturbative QCD suggests $c \gtrsim 0.3$
$a_2 = m_s^2 - 4\Delta^2$	the s-quark mass against the **gap** Δ of color superconductivity (CFL phase) — it can be negative
B	the **bag constant**: the cost of opening the QCD vacuum

At the surface $p = 0$, but the density is not: $\rho_s \approx 4B \sim 10^{14}$–$10^{15}$ g/cm^3. The star is **self-bound**: at small masses $M \propto R^3$, unlike a neutron star.

TOV + the tidal equation with the surface jump ($\Delta y = -4\pi R^3 \rho_s / M$), solved here. The paper's example gives 2.19 M⊙, 11.97 km and $\Lambda = 852$ — the panel reproduces it.

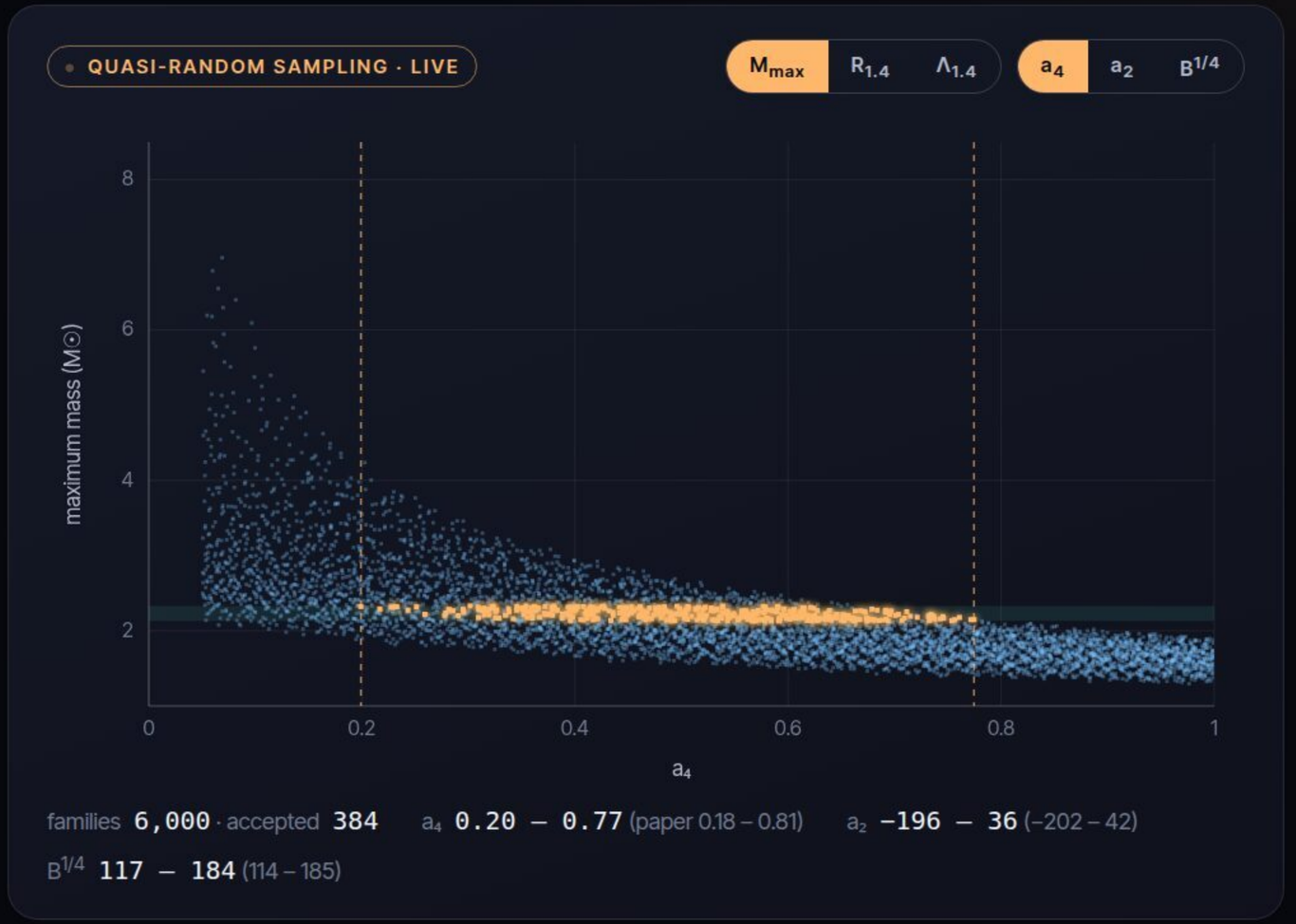


Thousands of stars, *drawn at random*

Each point (a_2, a_4, B) inside the stability window is a **whole family** of stars: TOV for M and R, the tidal equation for Λ. The paper drew **263,287** points by Latin hypercube sampling; here the browser draws its own, live.

	ACCEPTED RANGE	WHERE IT COMES FROM
M_{max}	2.13 – 2.33 M⊙	pulsars in binaries (Romani et al. 2022) · GW170817 + GRB 170817A (Rezzolla et al. 2018)
$R_{1.4}$	10.00 – 13.25 km	NICER radii — **ray tracing** — and gravitational waves (compilation by Pang et al. 2023)
$\Lambda_{1.4}$	< 970	tidal deformability from GW170817

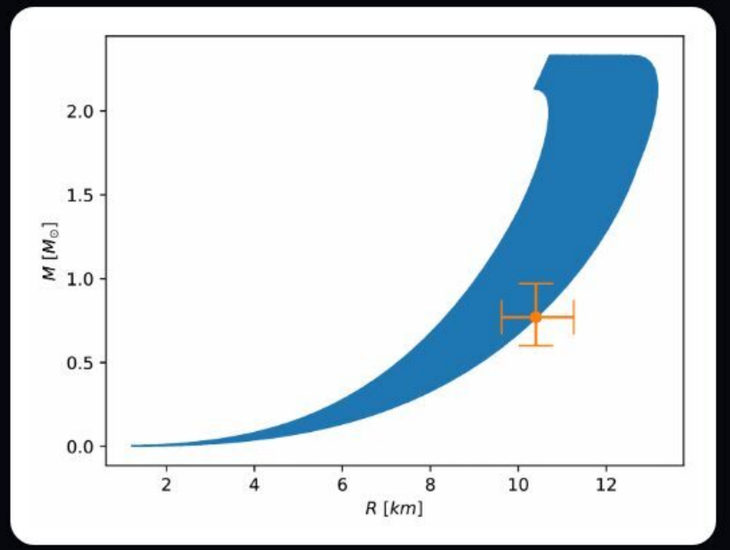
Amber: the families that pass all three tests. The dashed lines show how far the accepted ones reach — and they converge to the paper's limits.



Interacting quarks, a dense surface

COMBINED CONSTRAINTS	RANGE
a_4	0.18 – 0.81
a_2 (10^3 MeV^2)	−202 – 42
$B^{1/4}$ (MeV)	114 – 185
$R_{1.4}$ (km)	10.00 – 12.26
$\Lambda_{1.4}$	270 – 970
$\rho_{surface}$ (10^{15} g/cm^3)	0.29 – 0.60
c_s/c	0.51 – 0.85

The sound speed exceeds $c/\sqrt{3} \approx 0.58$ — the conformal limit of QCD at infinite density — when $a_2 < 0$.



All M–R curves that pass the constraints, with XMMU J173203.3−344518 (orange).

- $a_4 \lesssim 0.81$: the matter departs by at least **20%** from free quarks. Strong interactions cannot be neglected, at any mass.
- **$\Delta \lesssim 230$ MeV** (with $m_s = 100$ MeV), from the lower limit on a_2 — in line with the independent bound of $\lesssim 216$ MeV (Kurkela et al. 2024).
- **The surface jumps from vacuum to 1.1–2.2 ρ_{sat}**: a number that enters the tides, the oscillation modes and the star's mountains.
- **$R_{1.4}$ = 10.0–12.3 km**, like a neutron star: the radius alone cannot tell them apart; the tides can.
- **XMMU J1732−344** (0.77 M⊙, 10.4 km, in HESS J1731−347) falls on the curves effortlessly — a quark-star candidate, if the atmosphere model behind its radius is right.

PEREIRA, OTTONI, COELHO, RUEDA & DE LIMA · PRD 110, 103014 (2024)

When core and crust *do not spin together*

Almost every calculation treats a pulsar as a **rigid body**. But the interior may be superfluid, have a phase transition — a quark core — or gain accreted layers that spin differently, like the Sun's tachocline.

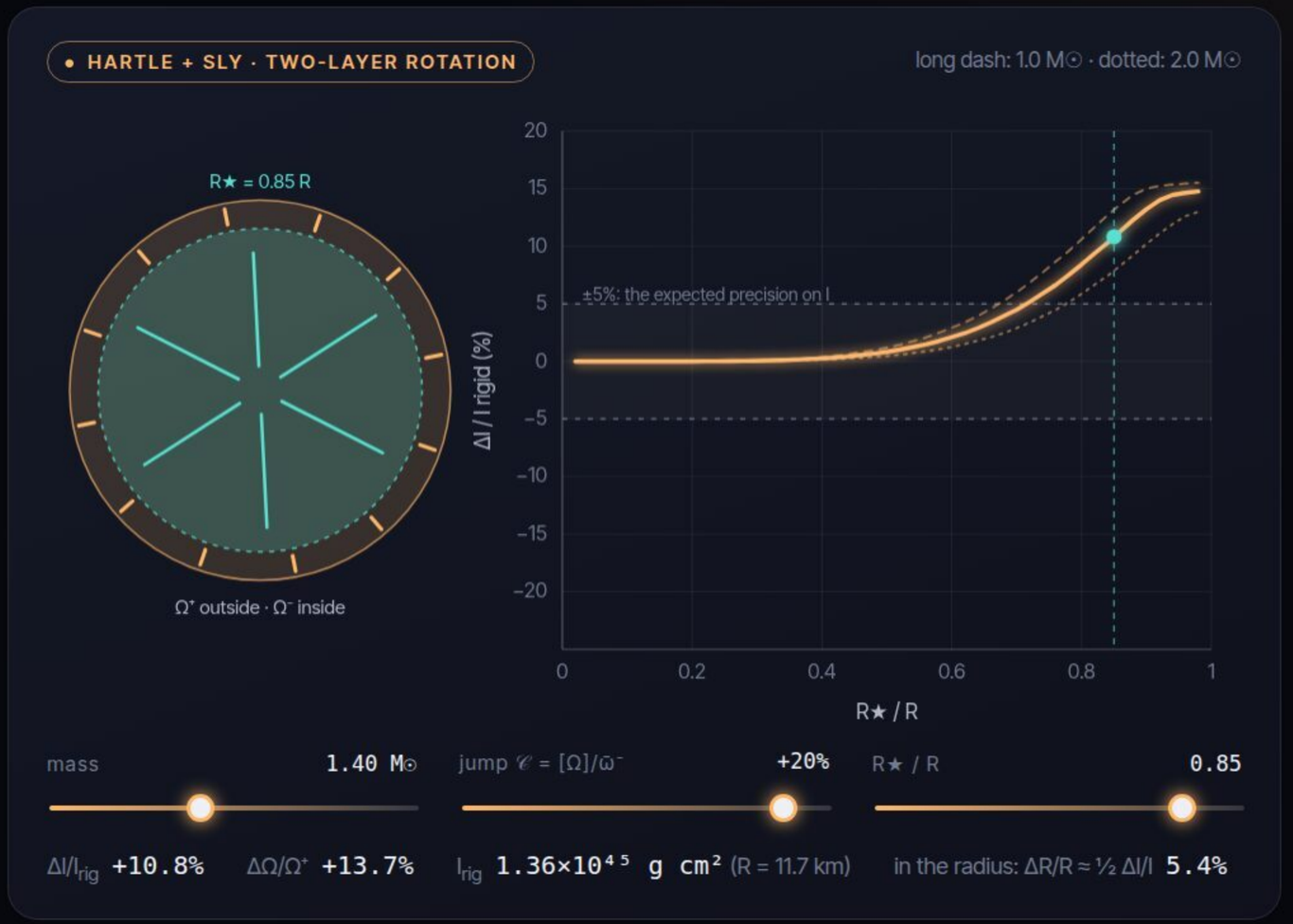
$$\frac{1}{r^4}\frac{d}{dr}(r^4 j\,\bar{\omega}') + \frac{4j'}{r}\,\bar{\omega} = 0$$

FRAME DRAGGING IN SLOW ROTATION · HARTLE 1967 · $\bar{\omega} = \Omega - \omega$

$$[\omega]_{R\star} = [\Omega],\ [\omega']_{R\star} = 0 \cdot I = \frac{J}{\Omega^+}$$

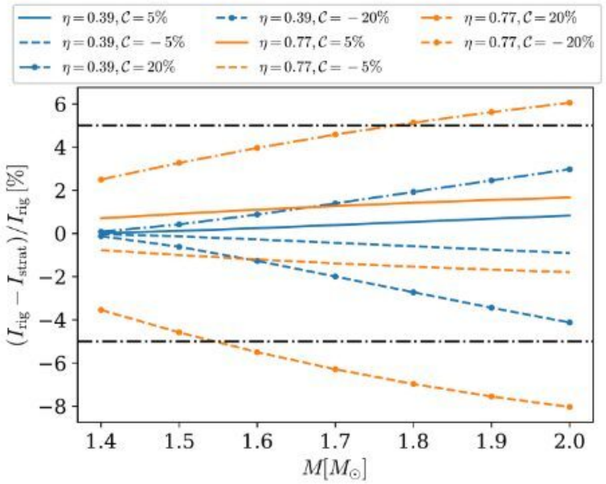
THE JUMP AT R★, DERIVED IN THE PAPER · Ω^+: THE SURFACE SPIN, THE ONE TIMING MEASURES

J comes from the derivative of $\bar{\omega}$ at the surface, so it **feels the jump**: the same star, with the same Ω^+, has a different moment of inertia.



Rigid rotation is an *assumption* — and it has a cost

- **Near the surface, $\Delta I/I \to \Delta\Omega/\Omega$**[+]; below ~40% of the radius the effect vanishes. It grows fast for $R\star \gtrsim 0.6$ R, and more in light stars.
- **Hybrid stars**: the jump sits at the transition to the quark core, and only exceeds 5% with $\mathscr{C}$ ~ 20% and $R\star \gtrsim 0.8$ R (figure).
- **In the radius**: with a known mass, $\Delta R/R = \frac{1}{2}\,\Delta I/I$. Ten percent in I is 5% in R — the size of the NICER error bars, which come from **ray tracing**.
- **Direct measurement of I**: the double pulsar J0737–3039A should give I to 11% by 2030 (today, I_{45} = 1.15–1.48). Jumps of 10–20% in Ω cannot be told from rigid rotation.
- **Energy**: with I 10–20% larger, five Fermi gamma-ray pulsars with $L_\gamma > \dot{E}$ fit back within the rotational energy.
- **I-Love-Q**: the quadrupole depends on another function besides J — the universal relations weaken. And in **CCOs**, accreted layers may spin differently for up to ~10 thousand years.



Hybrid stars (η = 0.39 and 0.77): Δ//I with the jump at the phase transition, against mass.

PULSAR (FERMI)	$L_\gamma/\dot{E}$, I_0	+10%	+20%
J1057–5851	1.19	> 1	0.99
J1522–5735	1.09	0.99	0.91
J1650–4601	1.11	> 1	0.92

CONCLUSIONS

From geometry *to observation* — and back

- In a neutron star, light bending, redshift and delays are **not corrections**: they define the image and the light curve.
- Backward ray tracing — with the exact integral when the compactness calls for it — links the metric to what a telescope measures.
- Applied to Chandra, XMM-Newton and NuSTAR data, it gave the mass, radius, field and spot geometry of magnetars and of an accreting star — and, through its spectrum, the temperature and height of its column.
- Since the light curve depends only on the exterior metric, it also **tests gravity**: scalar-tensor theories and braneworld.
- And the interior matters: **quark stars** and **stratified rotation** change the M, R and I that ray tracing measures.

NEXT STEPS

- Magnetised atmospheres and exact ray tracing together, for isolated cooling stars.
- Fast rotation and metrics beyond Schwarzschild in the same fits.
- Data from the next generation: eXTP, NewAthena, STROBE-X.

The panels in this seminar run in the browser: *rafael-lima.pages.dev/talks*.

IMAGE CREDITS

Freely licensed *photos and figures*

Albert Einstein — Ferdinand Schmutzer / Adam Cuerden · public domain

Karl Schwarzschild — unknown author · public domain

M87* (EHT) — Event Horizon Telescope Collaboration · CC BY 4.0

Sgr A* (EHT) — EHT Collaboration · CC BY 4.0

Jocelyn Bell, 1967 — Roger W Haworth · CC BY-SA 2.0

Antony Hewish — Woodruff T. Sullivan III / NRAO/AUI Archives (NRAO/AUI/NSF) · CC BY 4.0

Chart record of CP 1919, 1967 — Bill Thompson (Billthom) · CC BY-SA 4.0

Neutron star over Manhattan — NASA's Goddard Space Flight Center · public domain

1919 eclipse — ESO/Landessternwarte Heidelberg-Königstuhl/F. W. Dyson, A. S. Eddington, & C. Davidson · CC BY 4.0

SMACS 0723 (JWST) — NASA, ESA, CSA, and STScI · public domain

NICER — NASA · public domain

XMM-Newton — ESA/XMM-Newton · CC BY-SA 3.0 IGO

Chandra — NASA/CXC/NGST · public domain

Pulsar (illustration) — NASA · public domain

Magnetar (illustration) — ESO/L. Calçada · CC BY 4.0

Carl Brans — Cfbolner · CC BY-SA 4.0

Thibault Damour — Melirius · CC BY 3.0

PSR J0030+0451: hot-spot models — NASA's Goddard Space Flight Center · public domain

Paper figures (Part IV) — de Lima et al., ApJ 889, 165 (2020); de Lima et al., JHEAp 42, 52 (2024, CC BY 4.0 on arXiv); Silva et al., Galaxies 11, 18 (2023, CC BY 4.0); Ottoni et al., EPJC 84, 1337 (2024, CC BY 4.0); dos Santos Júnior, de Lima & Moraes, arXiv:2607.09836 (CC0); Pereira et al., PRD 110, 103014 (2024); Zastrow et al., PRD 112, 083010 (2025); Silva, de Lima, Coelho & de Araújo (submitted to JHEAp, 2026)

Simulated Sobral plate — positions from the Tycho-2 catalogue (Høg et al., A&A 355, L27, 2000), via VizieR/CDS

Be/X binary (illustration) — AI-generated

P–Ṗ diagram — ATNF pulsar catalogue 2.8.1 (Manchester et al., AJ 129, 1993, 2005)

THANK YOU

Questions?

Slides, animations and dashboards available at
rafael-lima.pages.dev/talks

Rafael C. R. de Lima

rafael.lima@udesc.br · rafael-lima.pages.dev